

Reactivity study of 3,3-dimethylbutanal and 3,3-dimethylbutanone: Kinetic, reaction products, mechanisms and atmospheric implications

Inmaculada Aranda¹, Sagrario Salgado^{1,2}, Beatriz Cabañas^{1,2}, Florentina Villanueva² and Pilar Martín^{1,2*}

¹Universidad de Castilla-La Mancha, Departamento de Química Física, Facultad de Ciencias y Tecnologías Químicas, Avda. Camilo José Cela s/n, 13071, Ciudad Real, Spain.

²Universidad de Castilla-La Mancha, Instituto de Investigación en Combustión y Contaminación Atmosférica (ICCA), Camino de los Moledores s/n, 13071, Ciudad Real, Spain.

*Corresponding author. Email address: mariapilar.martin@uclm.es

Abstract: 3,3-dimethylbutanal (33DMbutanal, (CH₃)₃CCH₂C(O)H) and 3,3-dimethylbutanone (33DMbutanone, (CH₃)₃CC(O)CH₃) are carbonyl compounds that could play a key role in tropospheric chemistry. To better understand the effects of carbonyl compounds in the atmosphere, a kinetic and mechanistic study was conducted on the degradation of 33DMbutanal and 33DMbutanone with atmospheric oxidants (Cl atoms, OH and NO₃ radicals). The kinetic experiments were performed at 710 ± 30 Torr and at room temperature (298 ± 5 K) using a relative method and FTIR (Fourier Transform Infrared Spectroscopy) to monitor the reactions. The rate coefficients (*k* in units of cm³ molecule⁻¹ s⁻¹) obtained were: *k*_{Cl+33DMbutanal} = (1.27 ± 0.08) × 10⁻¹⁰, *k*_{Cl+33DMbutanone} = (4.22 ± 0.27) × 10⁻¹¹, and *k*_{OH+33DMbutanone} = (1.265 ± 0.05) × 10⁻¹². The reaction products were also determined using FTIR and GC-MS (Gas Chromatography/Mass Spectrometry). The main products observed were carbonyl compounds, including acetone, formaldehyde and 2,2-dimethylpropanal. In the presence of NO, nitrated compounds were also formed, and at high NO₂ concentrations peroxyacetyl nitrate (PAN) and peroxy-3,3-dimethylbutyryl nitrate were clearly identified. Other unquantified compounds were multifunctional organic compounds and organic acid of low volatility. Both 33DMbutanal and 33DMbutanone degrade rapidly near emission sources with minimal impact on radiative forcing. However, they may contribute to tropospheric ozone, with a Photochemical Ozone Creation Potential (POCP)_E range of 15-69, and secondary organic aerosol formation, potentially worsening air quality and contributing to photochemical smog.

Con formato: Fuente: Cursiva, Color de fuente: Rojo

Con formato: Fuente: Cursiva, Color de fuente: Rojo

Con formato: Fuente: Cursiva, Color de fuente: Rojo

Con formato: Fuente: Cursiva, Color de fuente: Rojo

Con formato: Color de fuente: Rojo

Con formato: Color de fuente: Rojo

Con formato: Color de fuente: Rojo

Con formato: Color de fuente: Rojo

1 Introduction

Carbonyl compounds are a group of oxygenated volatile organic compounds (OVOCs) that are emitted into the atmosphere from natural and anthropogenic sources (Bao et al., 2022), but they are also formed in the atmosphere as oxidation products of other volatile organic compounds (VOCs) (Mellouki et al., 2015). It is well established that OVOCs play an important role in the sequence of chemical reactions that leads to their further oxidation and contributes to the tropospheric ozone formation in both polluted and remote environments with important effect on health as is the case of formaldehyde and acetaldehyde (Zhou et al., 2023; Liu et al., 2022; Calvert et al., 2011; Liu et al., 2022; Mellouki et al., 2015; Calvert et al., 2011; Zhou et al., 2023). In addition, large carbonyl compounds could influence on climate change altering the Earth's radiation balance if they are strong infrared light absorbers by altering the Earth's radiation balance and their atmospheric concentrations are sufficiently high. Additionally, carbonyls could be an important source of aerosol which could further affect radiation balance and be hazardous for health (Liu et al., 2022; Heald and Kroll, 2020; Liu et al., 2022).

The rising O₃ levels in mega-city clusters like Chinese cities underscore the critical need for effective control of ambient carbonyls, significant precursors of O₃. Moreover, as intermediate products of hydrocarbon oxidation, carbonyls likely play a pivotal role in minimizing the disparity between atmospheric reactivity in measurements and simulations. Previous studies (Zhou et al., 2023; Liu et al., 2022; Mellouki et al., 2015; Calvert et al., 2011) Calvert et al., 2011, Liu et al., 2022, Mellouki et al., 2015, Zhou et al., 2023 have provided valuable insights into carbonyls' presence, composition, origins, and impact on O₃ and SOA formation, using a combination of field measurements, numerical simulations, and laboratory experiments. Nevertheless, further research is still warranted to achieve a more comprehensive understanding of carbonyls' sources and sinks, given the complexity of their emission and degradation processes (Liu et al., 2022).

In this work, the tropospheric reactivity of two carbonyls compounds whose reactivity is not yet completely established, has been studied: 3,3-dimethylbutanal (33DMbutanal, (CH₃)₃CCH₂C(O)H) and 3,3-dimethylbutanone (33DMbutanone, (CH₃)₃CC(O)CH₃). These two carbonyls are among the reaction products identified in the atmospheric degradation of two alcohols (3,3-dimethyl-1-butanol and 3,3-dimethyl-2-butanol), whose reactivity have been previously studied (by our research group) (Colmenar et al., 2020). On the other hand, 33DMbutanal 3,3-dimethylbutanal has also been detected as reaction product in the reaction of 2,4,4-trimethyl-1-pentanol with Cl atoms (Vila et al., 2020) and it could be an intermediate in the synthesis of neotame, a sweetener (Tanielyan and Augustine, 2012). Industrially, 33DMbutanone, known as methyl tert-butyl ketone, is produced for use in fungicides, herbicides and pesticides (Liu et al., 2022) and it might also be used as a solvent for the extraction of methylphenols from wastewater (Xiong et al., 2018). Specifically, in the study of Byrne et al. (2018) 33DMbutanone has been identified as potential replacements for hazardous volatile non-polar solvents such as toluene, due to the low toxicity and good solvation characteristics. In addition to direct emissions, 33DMbutanone could be present in the atmosphere as a reaction product of the gas-phase oxidation of 2,2-dimethylbutane and 3,3-dimethyl-2-butanol (Saunders et al., 2003; Jenkin et al., 1997; Saunders et al., 2003) and 3,3-dimethyl-2-butanol (Colmenar et al., 2020).

Specifically, for 33DMbButanal and 33DMbutanone few studies about their atmospheric reactivity have been reported in the literature. In the case of the reaction of 33DMbutanal with OH radicals, the experimental rate coefficient has been measured by Aschmann et al. (2010) and D'Anna et al. (2001). Only one study on the reaction products with OH radicals has been reported by Aschmann et al. (2010). For the reaction of 33DMbButanal with

Con formato: Color de fuente: Rojo

Con formato: Color de fuente: Rojo

Con formato: Color de fuente: Rojo

Con formato: Color de fuente: Rojo

Con formato: Color de fuente: Rojo

Con formato: Color de fuente: Rojo

Con formato: Color de fuente: Rojo

Con formato: Color de fuente: Rojo

Con formato: Fuente: (Predeterminada) Times New Roman

Con formato: Color de fuente: Rojo

Con formato: Color de fuente: Rojo

Con formato: Color de fuente: Rojo

Con formato: Color de fuente: Rojo

Con formato: Color de fuente: Rojo

Con formato: Color de fuente: Rojo

Con formato: Color de fuente: Rojo

Con formato: Color de fuente: Rojo

Con formato: Color de fuente: Rojo

Con formato: Color de fuente: Rojo

Con formato: Color de fuente: Rojo

67 NO₃ radicals two kinetic studies are available in the literature (D'Anna et al., 2001; D'Anna and Nielsen 1997).
68 Tadic et al., 2012 has reported the photochemical parameters of 33DMbutanal due to the importance of the
69 photodissociation of aldehydes in the atmosphere since it could represent an important source of free radicals. To
70 our knowledge, there are no data about the reaction of 33DMbutanal with Cl atoms.

71 In the case of 33DMbutanone only a kinetic study with Cl atoms has been carried out (Farrugia et al., 2015) and
72 two studies with OH radicals (Mapelli et al., 2023; Wallington and Kurylo 1987). In the studies of OH radicals, the
73 rate coefficient has been obtained at different temperatures and at low pressure, using absolute methods. No studies
74 have been carried out on the reaction products of Cl atoms and OH radicals reaction with 33DMbButanone that
75 could help to establish the reaction mechanisms.

76 Taking the above into consideration, the aim of this work is to complete the studies about the reactivity of
77 33DMbButanal and 33DMbButanone to further understand their atmospheric chemistry in particular and the
78 carbonyls reactivity in general. For this purpose, the kinetic study has been conducted for the reactions of
79 33DMbButanal and 33DMbButanone with Cl atoms and 33DMbButanone with OH radicals using a relative method
80 and FTIR (Fourier Transform Infrared Spectroscopy) technique as detection system. Additionally, for the reactions
81 of 33DMbButanal with Cl atoms, OH and NO₃ radicals and for the reactions of 33DMbButanone with Cl atoms and
82 OH radicals a complete reaction product study has been performed using FTIR and GC-MS (Gas
83 Chromatography/Mass Spectrometry) techniques. This work is to date the first kinetic study reported in bibliography
84 for the reaction of 33DMbButanal with Cl atoms and the first study on reaction products and mechanisms for the
85 reactions of 33DMbButanone with Cl atoms and OH radicals, and 33DMbButanal with Cl atoms and NO₃ radicals.
86 Additionally, this work includes a study on the reaction products for the reaction of 33DMbButanal with OH radicals
87 in order to confirm the mechanism proposed by Aschmann et al. (2010).

88 2 Experimental Section

89 2.1 Rate coefficients determination: relative method

90 Rate coefficients have been determined using a relative rate method on the assumption that the organic compound
91 (carbonyl: 33DMbButanal or 33DMbutanone), and the reference compound (R) are removed solely by their
92 reactions with the oxidants (Ox: Cl or ·OH):



95 where k_{carbonyl} and k_{R} are the rate coefficients of the carbonyl and the reference compound, respectively. The kinetic
96 treatment for the reactions (R1) and (R2) gives the following relationship:

97
$$\ln \left(\frac{[\text{carbonyl}]_0}{[\text{carbonyl}]_t} \right) = \frac{k_{\text{carbonyl}}}{k_{\text{R}}} \times \ln \left(\frac{[\text{R}]_0}{[\text{R}]_t} \right) \quad (I)$$

98 where [carbonyl]₀, [R]₀, [carbonyl]_t, [R]_t, are the initial concentrations and those at time t for the carbonyl and the
99 reference compound, respectively. At least three reference compounds were employed for each studied reaction, and
100 the experiments were performed in triplicate for each one. According to Eq. (I), a plot of ln([carbonyl]₀/[carbonyl]_t)
101 versus ln([R]₀/[R]_t) (or a proportional property) should give a linear fit with an intercept equal to zero. The slope of

Con formato: Color de fuente: Rojo

Con formato: Color de fuente: Rojo

Con formato: Color de fuente: Rojo

Con formato: Color de fuente: Rojo

Con formato: Color de fuente: Rojo

Con formato: Color de fuente: Rojo

Con formato: Color de fuente: Rojo

Con formato: Color de fuente: Rojo

Con formato: Color de fuente: Rojo

Con formato: Color de fuente: Rojo

Con formato: Color de fuente: Rojo

Con formato: Color de fuente: Rojo

Con formato: Color de fuente: Rojo

Con formato: Color de fuente: Rojo

Con formato: Color de fuente: Rojo

Con formato: Fuente: Cursiva, Color de fuente: Rojo

Con formato: Color de fuente: Rojo

Con formato: Fuente: Cursiva, Color de fuente: Rojo

Con formato: Color de fuente: Rojo

Con formato: Fuente: Cursiva, Color de fuente: Rojo

Con formato: Fuente: Cursiva, Color de fuente: Rojo

Con formato: Color de fuente: Rojo

Con formato: Color de fuente: Rojo

the plot corresponds to the ratio of the rate coefficients ($k_{\text{carbonyl}}/k_{\text{R}}$). Therefore, the value of k_{carbonyl} can be determined if the rate coefficient of the reference compound (k_{R}) is known.

2.2 Experimental systems and procedure

Experimental details can be found in previous publications (Aranda et al., 2021; Colmenar et al., 2024, Colmenar et al., 2018, 2020, a, 2018). Therefore, only a brief description is provided here.

Kinetic and product studies were performed at room temperature (298 ± 5 K) and atmospheric pressure (710 ± 18 Torr) employing a 50 L Pyrex® glass cell as reaction chamber, coupled to a FTIR spectrometer (Thermo, Nicolet 6700). The gas cell contains a multireflection system that allows a maximum optical path of 200 m (Saturn Series Multi-Pass cell). For the FTIR spectra collection, a total of 60 interferograms were co-added over 98 s, usually taken in the range of $650\text{--}4000\text{ cm}^{-1}$ with a resolution of 1 cm^{-1} . Additionally, for product identification, samples of the reaction mixture were collected via a port on the gas cell taken using a Solid Phase MicroExtraction (SPME) fiber (DVB/CAR/PDMS) as the pre-concentration passive sampling method. After the adsorption process (5–8 minutes), the fiber was transferred to the injection port of the gas chromatograph (GC) coupled to a Time-of-Flight Mass Spectrometer analyzer (MSTOF, AccuTOF GCv/Jeol). In the injection port of the gas chromatograph, where the compounds were desorbed at $250\text{ }^{\circ}\text{C}$, separated and detected by GC-MSTOF, and carried to a Gas Chromatograph coupled to a Mass Spectrometer with Time Of Flight analyzer (GC-MSTOF) (AccuTOF GCv/Jeol). Experimental details can be found in previous publications (Aranda et al., 2020, Aranda et al., 2024, Colmenar et al., 2018, 2020a, 2020b). Therefore, only a brief description is provided.

For FTIR experiments, the Pyrex® gas cell used contains a multireflection system that allows a maximum optical path of 200 m (Saturn Series Multi-Pass cell). For the FTIR spectra collection, a total of 60 interferograms were co-added over 98 s, usually taken in the range of $650\text{--}4000\text{ cm}^{-1}$ with a resolution of 1 cm^{-1} . The After the adsorption process (5–8 minutes of adsorption), the fiber was taken to the injection port of the gas chromatograph (GC), where the compounds were desorbed at $250\text{ }^{\circ}\text{C}$, separated and detected by GC-MSTOF. Two different capillary columns with the same characteristics were used: a TRB-1701 (Teknokroma, $30\text{ m} \times 0.32\text{ mm} \times 1\text{ }\mu\text{m}$) and a Equity™ – 1701 (Supelco, $30\text{ m} \times 0.32\text{ mm} \times 1\text{ }\mu\text{m}$). Once in the mass spectrometer, the compounds were ionized (Electron Ionization (EI) and/or Field Ionization (FI)) and fragmented to obtain their mass spectrum (MS). The chromatographic conditions used for the analysis were as follows: injection port, $250\text{ }^{\circ}\text{C}$; interface, $250\text{ }^{\circ}\text{C}$; oven initial temperature of $40\text{ }^{\circ}\text{C}$ for 4 min; ramp, $25\text{ }^{\circ}\text{C min}^{-1}$ to $120\text{ }^{\circ}\text{C}$, held for 10 min; second ramp, $20\text{ }^{\circ}\text{C min}^{-1}$ to $200\text{ }^{\circ}\text{C}$, held for 2 min.

The oxidants were generated by photolysis or decomposition of a precursor (Finlayson-Pitts and Pitts 2000), ($\lambda=350\text{ nm}$) of molecular chlorine (Cl_2) for reactions with Cl atoms and by methyl nitrite (CH_3ONO) in the presence of O_3 and NO , for reactions with OH radicals. Some experiments have been carried out using H_2O_2 as precursor of OH and UV radiation ($\lambda=254\text{ nm}$) in a Quartz gas cell reactor.

The decomposition of dinitrogen pentoxide was used as source of NO_3 radical according to reaction 1:

$\text{N}_2\text{O}_5 + \text{M} \rightarrow \text{NO}_2 + \text{NO}_3 + \text{M}$ (R1) The generation of Cl atoms was achieved through the photolysis of Cl_2 using radiation emitted by actinic lamps ($\lambda_{\text{max}} = 360\text{ nm}$).

$\text{Cl}_2 + h\nu \rightarrow 2\text{ Cl}$ (R3)

Con formato: Fuente: Cursiva, Color de fuente: Rojo

Con formato: Fuente: Cursiva, Color de fuente: Rojo

Con formato: Fuente: Cursiva, Color de fuente: Rojo

Con formato: Fuente: Cursiva, Color de fuente: Rojo

Con formato: Color de fuente: Rojo

Con formato: Color de fuente: Rojo

Con formato: Color de fuente: Rojo

Con formato: Color de fuente: Rojo

139 Hydroxyl radicals ($\cdot\text{OH}$) were generated by the photolysis of methyl nitrite (CH_3ONO) in air in the presence of NO ,
140 following the reaction sequence below:



144 Some experiments have been carried out using H_2O_2 as precursor of OH and UV radiation ($\lambda=254\text{ nm}$) in a Quartz
145 gas cell reactor.



147 Nitrate radicals ($\text{NO}_3\cdot$) were generated through the thermal decomposition of dinitrogen pentoxide (N_2O_5) at room
148 temperature, according to the following equilibrium



151 The kinetic experiments were conducted in a nitrogen atmosphere for reactions with Cl atoms, while synthetic air
152 was used for reactions with OH radicals. All the experiments conducted for the study of products were carried out
153 in synthetic air and in the absence of the reference compound.

154 The reactions were followed by measuring the absorbance of the characteristic IR bands of each organic compound
155 (33DMbutanal/33DMbutanone and the reference compounds in the case of kinetic analysis) at different reaction
156 times. The IR spectra were processed using OMNIC software, thought a subtraction procedure (elimination) of the
157 IR bands.

158 The concentration ranges (in ppm) used in the kinetic experiments were: 10-12 for 33DMbutanal and
159 33DMbutanone, 9-10 for 1-butene, 10-14 for propene, 35-40 for 2-methylpropene, 13-14 for isopropanol, 10-17
160 for cyclohexane, 5-14 for propanal, 9-10 for 2-methyl-2-butanol, 5-6 for ethyl formate, 11-15 for 1-butanol,
161 17-22 for Cl_2 , 15-20 for NO and 16-20 for methyl nitrite. In the case of the reaction product experiments, the typical
162 concentration (in ppm) was: 10-14 for 33DMbutanal and 33DMbutanone; 22 for Cl_2 , 15-20 for NO , 16-20 for methyl
163 nitrite, 30 for H_2O_2 and for 14-25 for N_2O_5 .

164 2.3 Materials

165 Information on the purity and supplier company of the reagents used to carry out the experiments is specified below:
166 33DMbutanal (95%), 33DMbutanone (97%), and the reference compounds: 1-butene and propene ($\geq 99\%$), 2-
167 methylpropene ($\geq 99.5\%$), isopropanol (70% in H_2O), propanal (97%), cyclohexane (99.5%), 2-methyl-2-
168 butanol ($\geq 99\%$), ethyl formate (97 %), 1-butanol ($\geq 99\%$), 2,2-dimethylpropanoic acid (99%), 3,3-
169 dimethylbutanoic acid (98%) from Sigma Aldrich. Acetone ($\geq 99.5\%$) from Supelco. 2,2-
170 dimethylpropanal (22DMpropanal) ($>95\%$) from TCI. The precursors of the radicals were: methyl nitrite, CH_3ONO ,
171 synthesized in the laboratory according to the method of Taylor et al., (1980) and Cl_2 (99%) from Praxair. NO
172 (98.5%) from Air Liquide, H_2O_2 (50 wt. % in H_2O , stabilized) from Sigma Aldrich. N_2 (99.999%) and synthetic air

Con formato: Justificado, Interlineado: 1,5 líneas

Con formato: Color de fuente: Rojo

Con formato: Color de fuente: Rojo

Con formato: Color de fuente: Rojo

Con formato: Color de fuente: Rojo

Con formato: Color de fuente: Rojo

Con formato: Color de fuente: Rojo

Con formato: Color de fuente: Rojo

Con formato: Color de fuente: Rojo

Con formato: Color de fuente: Rojo

Con formato: Color de fuente: Rojo

(99.999%) from Praxair. Dinitrogen pentoxide (N₂O₅) synthesized in the laboratory according to the procedure described by Schott and Davids (1958).

3 Results and discussion

3.1 Kinetic study

The reference compounds have been selected according to the following conditions: first that at least one active IR band does not overlap with those of the compound under study (33DMbutanal or 33DMbutanone) and second, that $0.1 \leq k_{\text{carbonyl}}/k_{\text{R}} \leq 10$. In addition, a series of experiments was carried out in order to evaluate possible heterogeneous reactions with the walls, reactions between the compound under study and the reference compound, photolysis of any of them and/or reactions with the oxidant precursor. *To determine these loss processes, the initial spectrum of the reactants was compared with the spectrum recorded after a long period (45 minutes, which is the typical time range for the kinetic study).* The results of these experiments showed that *under the experimental conditions used in this work,* the losses of the reactants due to these processes were negligible (< 3% photolysis *and/or dark lossless* in the case of 33DMbutanal and 0% for 33DMbutanone).

The IR absorption bands used to follow the evolution of the different compounds were: 33DMbutanal, 2700 cm⁻¹; 1-butene, 911 cm⁻¹; propene, 878-942 cm⁻¹; 2-methylpropene, 912 cm⁻¹; *isopropanol*, 1070 and 1251 cm⁻¹; cyclohexane, 2862 and 2933 cm⁻¹; 33DMbutanone, 1137 cm⁻¹; propanal, 2710 cm⁻¹; 2-methyl-2-butanol, 883 cm⁻¹; ethyl formate, 1192 and 1194 cm⁻¹; 1-butanol, 1060 cm⁻¹.

The plots of $\ln([\text{carbonyl}]_0/[\text{carbonyl}]_t)$ versus $\ln([R]_0/[R]_t)$ for each reaction were generated according to Eq. (I). As an example, *Figure 1* shows the plot of this equation for the reaction of 33DMbutanal with Cl atoms, along with *two of the* reference compounds used. At least three reference compounds were used for each reaction, to ensure the accuracy of the determined value. The reference compounds used and the values of their rate coefficients are included in Table 1. *These values correspond to those recommended by McGillen et al., (2020).*

Con formato: Fuente: Cursiva, Color de fuente: Rojo

Con formato: Fuente: Cursiva, Color de fuente: Rojo

Con formato: Color de fuente: Rojo

Con formato: Color de fuente: Rojo

Con formato: Color de fuente: Rojo

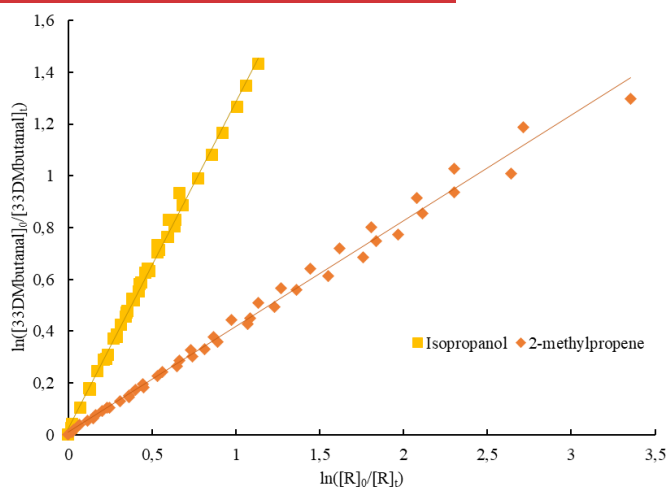
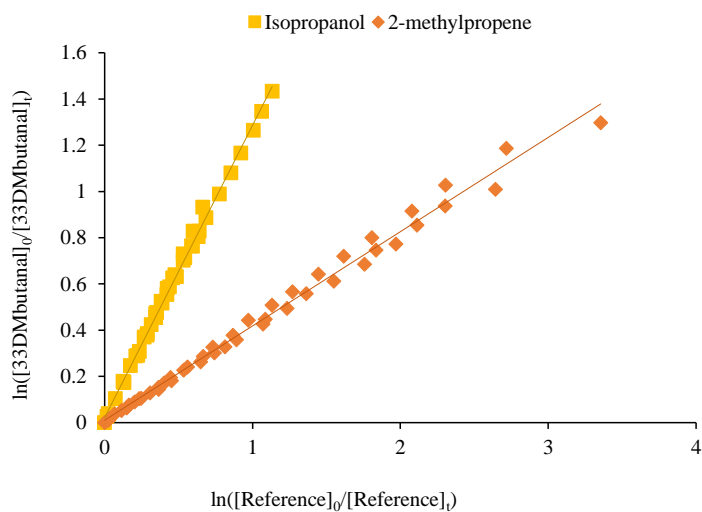


Figure 1. Plots of Eq. (I) for the reaction of 33DMbutanal with Cl atoms using two reference compounds.

The slopes of the plots correspond to the relationship k_{carbonyl}/k_R , knowing the value of k_R , the rate coefficients of carbonyls can be determined. It can be seen the good linear fit with an intercept close to zero, indicating the absence of secondary reactions. The plots for the reaction of 33DMbutanal with Cl atoms using cyclohexane as a reference, is presented in Fig. 1Sa. Additionally, the Fig. 1S includes the plots for the reaction of 33DMbutanal with Cl atoms

Con formato: Color de fuente: Rojo

Con formato: Color de fuente: Rojo

Con formato: Fuente: Cursiva, Color de fuente: Rojo

Con formato: Fuente: Cursiva, Color de fuente: Rojo

Con formato: Fuente: Cursiva, Color de fuente: Rojo

203 and OH radicals, along with all the reference compounds used. The plots show a linear fit with $r^2 \sim 0.99$ and low
204 origin intercept values, indicating the absence of secondary reactions. The $k_{\text{carbonyl}}/k_{\text{R}}$ and k_{carbonyl} obtained are shown
205 in Table 1.

Con formato: Fuente: Cursiva, Color de fuente: Rojo

Con formato: Fuente: Cursiva, Color de fuente: Rojo

Con formato: Fuente: Cursiva, Color de fuente: Rojo

Table 1. Summary of relative and absolute rate coefficients for the reaction of 33DMbutanal with Cl atoms and 33DMbutanone with Cl atoms and OH radicals. ***k* in units of $\text{cm}^3 \cdot \text{molecule}^{-1} \cdot \text{s}^{-1}$.**

Reaction	Reference compound ^a	$k_{\text{carbonyl}}/k_{\text{R}} \pm 2\sigma$	$^b k_{\text{carbonyl}} \pm 2\sigma_{\text{abs}}^{\text{c}}$
33DMbutanal+Cl ^a	2-methylpropene	0.38±0.01	1.26 ± 0.27
	$^a k_{\text{Cl}} = (-3.3 \pm 0.7) \times 10^{-10}$	0.40±0.01	1.32 ± 0.28
		0.44±0.01	1.46 ± 0.31
	Isopropanol	1.38±0.02	1.20 ± 0.31
	$^a k_{\text{Cl}} = (-0.87 \pm 0.23) \times 10^{-10}$	1.25±0.02	1.09 ± 0.28
		1.27±0.02	1.11 ± 0.29
	Cyclohexane	0.43±0.01	1.42 ± 0.22
	$^a k_{\text{Cl}} = (-3.3 \pm 0.5) \times 10^{-10}$	0.36±0.01	1.19 ± 0.18
Weighted Average			1.27 ± 0.08
33DMbutanone+Cl ^b	Reference compound	$k_{\text{carbonyl}}/k_{\text{R}} \pm 2\sigma$	$^d k_{\text{carbonyl}} \pm 2\sigma$
	Propanal	0.41 ± 0.02	5.10 ± 1.06
	$^a k_{\text{Cl}} = (-12.5 \pm 2.5) \times 10^{-11}$	0.37 ± 0.01	4.62 ± 0.93
		0.42 ± 0.01	5.22 ± 1.06
		0.42 ± 0.01	5.31 ± 1.07
	2-methyl-2-butanol	0.42 ± 0.01	3.03 ± 0.76
	$^a k_{\text{Cl}} = (-7.30 \pm 1.80) \times 10^{-11}$	0.43 ± 0.01	3.10 ± 0.78
		0.47 ± 0.01	3.40 ± 0.85
	Isopropanol	0.51 ± 0.02	4.41 ± 1.16
	$^a k_{\text{Cl}} = (-8.7 \pm 2.3) \times 10^{-11}$	0.48 ± 0.02	4.21 ± 1.10
		0.49 ± 0.01	4.22 ± 1.10
	Ethyl formate	4.87 ± 0.36	4.97 ± 1.05
	$^a k_{\text{Cl}} = (-1.0 \pm 0.2) \times 10^{-11}$	4.93 ± 0.18	5.03 ± 1.02
Weighted Average			4.22 ± 0.27
33DMbutanone+OH ^e	Reference compound	$k_{\text{carbonyl}}/k_{\text{R}} \pm 2\sigma$	$^d k_{\text{carbonyl}} \pm 2\sigma$
	Isopropanol	0.27 ± 0.01	1.39 ± 0.15
	$^a k_{\text{OH}} = (-5.2 \pm 0.5) \times 10^{-12}$	0.22 ± 0.01	1.17 ± 0.12
		0.23 ± 0.02	1.18 ± 0.12
	2-methyl-2-butanol	0.49 ± 0.03	1.67 ± 0.51
	$^a k_{\text{OH}} = (-3.4 \pm 1.0) \times 10^{-12}$	0.40 ± 0.02	1.38 ± 0.42
		0.56 ± 0.03	1.92 ± 0.59
	1-butanol	0.14 ± 0.01	1.27 36 ± 0.208
	$^a k_{\text{OH}} = (-9.18 \pm 2.0) \times 10^{-12}$	0.16 ± 0.01	1.50 62 ± 0.2434
		0.18 ± 0.01	1.68 0.96 ± 0.2611
	Cyclohexane	0.18 ± 0.01	1.23 ± 0.13
	$^a k_{\text{OH}} = (-6.7 \pm 0.7) \times 10^{-12}$	0.15 ± 0.01	1.00 ± 0.11
		0.25 ± 0.03	1.67 ± 0.26
Weighted Average			1.26 5 ± 0.05

^{a-b-c} k_{carbonyl} and k_{R} is given in 10^{-10} , 10^{-11} , 10^{-12} , respectively. The data of k_{R} (in units of $\text{cm}^3 \cdot \text{molecule}^{-1} \cdot \text{s}^{-1}$) are values recommended by McGillen et al., (2020). k_{carbonyl} (in units of $\text{cm}^3 \cdot \text{molecule}^{-1} \cdot \text{s}^{-1}$) is given in $^b 10^{-10}$, $^c 10^{-11}$, $^d 10^{-12}$. The quoted errors in the $k_{\text{carbonyl}}/k_{\text{R}}$, (2σ), are twice the statistical errors from the regression analysis ($2 \times \sigma_{\text{slope}}$). The total absolute error $\sigma(k_{\text{carbonyl}})$ is a combination of the statistical errors from the regression analysis (σ_{slope}) and the quoted error in the value of the rate coefficient of the reference compound (σ_{R}). The final values of the rate coefficients and the associated error were calculated as weighted average (Colmenar et al., 2020).

Con formato: Fuente: Cursiva, Color de fuente: Rojo

Con formato: Fuente: Cursiva, Color de fuente: Rojo

Con formato: Color de fuente: Rojo, Superíndice

Con formato: Fuente: Cursiva, Color de fuente: Rojo

Tabla con formato

Con formato: Superíndice

Con formato: Fuente: Cursiva, Color de fuente: Rojo

Con formato: Superíndice

Con formato: Fuente: Cursiva, Color de fuente: Rojo

Con formato: Derecha: -0,19 cm

Con formato: Color de fuente: Rojo, Superíndice

Con formato: Fuente: Cursiva, Color de fuente: Rojo

Con formato: Color de fuente: Rojo

Con formato: Color de fuente: Rojo, Superíndice

Con formato: Fuente: Cursiva, Color de fuente: Rojo

Con formato: Fuente: Cursiva, Color de fuente: Rojo

Con formato

Con formato: Color de fuente: Rojo

Con formato: Fuente: Cursiva, Color de fuente: Rojo

Con formato: Color de fuente: Rojo

Con formato: Fuente: Cursiva, Color de fuente: Rojo

Con formato: Fuente: Sin Cursiva

Con formato: Fuente: Cursiva, Color de fuente: Rojo

Con formato: Fuente: Cursiva, Color de fuente: Rojo

Con formato: Derecha: -0,19 cm

Con formato: Color de fuente: Rojo

Con formato: Color de fuente: Rojo

Con formato: Fuente: Cursiva, Color de fuente: Rojo

Con formato: Color de fuente: Rojo

Con formato: Color de fuente: Rojo

Con formato: Color de fuente: Rojo

Con formato: Color de fuente: Rojo

Con formato: Fuente: Cursiva, Color de fuente: Rojo

Con formato: Color de fuente: Rojo

Con formato: Color de fuente: Rojo

Con formato: Fuente: Cursiva

Con formato: Superíndice

Con formato: Superíndice

Con formato: Superíndice

214

215 To the best of our knowledge, this is the first work where the rate coefficient for the reaction of 33DMbutanal with
216 Cl atoms is determined. On the other hand, the values of the rate coefficients of the reaction of 33DMbutanone with
217 Cl atoms and OH radicals have been previously been determined with values of $(0.48 \pm 0.05) \times 10^{-10} \text{ cm}^3 \text{ molecule}^{-1} \text{ s}^{-1}$ (Farrugia et al., 2015) for Cl reactions and $(1.21 \pm 0.05) \times 10^{-12} \text{ cm}^3 \text{ molecule}^{-1} \text{ s}^{-1}$ (Wallington and Kurylo,
218 1987) and $(1.2 \pm 0.2) \times 10^{-12} \text{ cm}^3 \text{ molecule}^{-1} \text{ s}^{-1}$ (Mapelli et al., 2023) for OH reaction. These data are in good
219 agreement with the values obtained in this study, thereby contributing to the accurate determination of the rate
220 coefficients.
221

222 In the case of 33DMbutanone reactions, the rate coefficient for Cl reactions ($4.22 \times 10^{-11} \text{ cm}^3 \text{ molecule}^{-1} \text{ s}^{-1}$) is one
223 order of magnitude higher than the corresponding to OH reactions ($1.25 \times 10^{-12} \text{ cm}^3 \text{ molecule}^{-1} \text{ s}^{-1}$). This is the
224 general trend observed in the atmospheric chemistry for the oxidation reactions of organic compounds;
225 $k_{\text{Cl}} > k_{\text{OH}} > k_{\text{NO}_3}$ (Mellouki et al., 2015; Calvert et al., 2011; Atkinson, 2007). This behaviour can be explained by the
226 higher reactivity and lower selectivity of Chlorine atoms compared to the OH radicals, where the site of attack
227 determines its reactivity (Colmenar et al., 2020).

228 In Table 2, the rate coefficients for the reaction of different aldehydes and ketones in the butyl series with the main
229 atmospheric oxidants have been tabulated to analyse the influence of the ramifications on reactivity.

230

Con formato: Color de fuente: Rojo

Con formato: Fuente: Cursiva, Color de fuente: Rojo

Con formato: Fuente: Cursiva, Color de fuente: Rojo

Con formato: Fuente: Cursiva, Color de fuente: Rojo

Con formato: Color de fuente: Rojo

Con formato: Color de fuente: Rojo

Table 2. Rate coefficients for aldehydes and ketones in the butyl series with key atmospheric oxidants. k in units of $\text{cm}^3 \text{ molecule}^{-1} \text{ s}^{-1}$.

Aldehydes			
Compounds	k_{Cl}^a	k_{OH}^b	$k_{\text{NO}_3}^c$
Butanal	1.66 ± 0.4^d	23.7 ± 5^d	1.10 ± 0.4^d
2-methylbutanal	2.16 ± 0.32^e	33.3 ± 13^d	2.67 ± 0.8^d
3-methylbutanal	2.07 ± 0.14^f	25.9 ± 5^d	2.19 ± 0.7^d
3,3-dimethylbutanal	1.27 ± 0.08^g	21.4 ± 9^d	1.77 ± 0.4^d
Ketones			
Compounds	k_{Cl}^a	k_{OH}^b	$k_{\text{NO}_3}^c$
2-butanone	0.40 ± 0.16^d	1.05 ± 0.2^d	
3-methylbutanone	0.68 ± 0.07^d	3.00 ± 1.2^d	$< 0.05^h$
3,3-dimethylbutanone	0.48 ± 0.05^d	1.21 ± 0.5^d	
	0.42 ± 0.03^g	1.26 ± 0.1^g	
		1.2 ± 0.2^i	

^a k_{Cl} (in units of $\text{cm}^3 \text{ molecule}^{-1} \text{ s}^{-1}$), in 10^{-10} , 10^{-12} , 10^{-14} , respectively. ^dValues recommended in McGillen 2020. ^eAsensio et al., 2022. ^fBo et al., 2022. ^gThis work. ^hGlasius et al., 1997. ⁱMapelli et al., 2023

For butanals, the trend in rate coefficient values indicates that the presence of a methyl group influences to the reactivity, resulting in an increase in the rate coefficient compared to the compound without a methyl group. This could be attributed to the activation of the hydrogen atom at the α - position by a methyl group, as noted in the literature (Mellouki et al., 2015). Furthermore, the reactivity is influenced by both the position and quantity of methyl groups. Consequently, the activating influence exerted by the methyl group on the hydrogen bonded to the carbon adjacent to the aldehyde (α - position) is less pronounced when the methyl group occupies position 3 as opposed to position 2. Basically, the impact of the methyl group manifests as a short-range activating effect. Regarding the impact of the number of methyl groups on reactivity, in the case of 33DMbutanal, the significant decrease in the value of rate coefficient with respect to 3-methylbutanal could be explained by an increase in steric hindrance, making the hydrogen abstraction process at the α - position less probable, thereby resulting in lower reactivity compared to the compound with one methyl group (3-methylbutanal). The decrease in the rate coefficient may also be related to the fact that many of the abstractable hydrogens are now primary.

Concerning butanones, no data are available for reactions with NO_3 radicals, with only one value for the upper limit of 3-methylbutan-2-one (Glasius et al., 1997). The fact that the reactions of ketones with NO_3 radicals are too slow complicates their experimental study and therefore, the determination of their rate coefficients. The available data of rate coefficients for reactions of butanones with Cl atoms and OH radicals, show again that the presence of a methyl group attached to a carbon in the α - position with respect to the carbonyl group activates the abstraction of one hydrogen atom from this carbon, resulting in an increase of the rate coefficient. A comparison of rate coefficients for 2-butanone and 3-methylbutan-2-one reveals this effect, particularly pronounced in OH reactions. The presence of two methyl groups (33DMbutanone) produces a significant decrease in the value of the rate coefficient, which can be attributed to steric hindrance and a reduction in the number of secondary/tertiary abstractable hydrogens, that again could be explained by steric hindrance.

As can be observed in Table 2, the type of carbonyl group (aldehyde or ketone) also exerts a significant influence on the reactivity. The rate coefficients are generally one or two orders of magnitude higher for the aldehyde reactions compared to the reaction of ketones. The different reactivity of aldehydes and ketones with the main atmospheric

Con formato: Izquierda, Interlineado: Múltiple 1,08 lín.

Con formato: Superíndice

Con formato: Fuente: Cursiva

Con formato: Fuente: Cursiva

Con formato: Fuente: Cursiva

Con formato: Fuente: Cursiva

Con formato: Fuente: Cursiva

Con formato: Fuente: Cursiva

Con formato: Fuente: Cursiva

Con formato: Superíndice

Con formato: Superíndice

Con formato: Superíndice

oxidants has extensively been studied and documented in the literature (McGillen et al., 2020; Mellouki et al., 2015). The different reactivity observed in the reactions of atmospheric oxidant radical with saturated carbonyl compounds that are initiated by hydrogen abstraction, are due to the presence in the carbonyl compound of different types of hydrogens. In the aldehydic compounds there are two types of hydrogens that can be abstracted, the hydrogen directly attached to the carbonyl group (aldehydic hydrogen) and the hydrogen attached to the alkyl group (alkyl hydrogen), while in a ketone only alkyl hydrogens are present. The available kinetic and mechanistic data on the atmospheric degradation indicate that the H atom abstraction from the aldehydic group (–CHO) is more favoured than H atom abstraction from the C–H bonds of the alkyl chain. The rate coefficients obtained in this study for 33DMbutanal and 33DMbutanone confirm this argument.

Con formato: Color de fuente: Rojo

Additionally, it is well known that functional groups exert an activating or deactivating effect on reactivity, depending on the type of groups. The reactivity factors ($F(R)$; R =functional group) associated with the functional group to which a type of carbon is attached (primary (k_{prim}), secondary (k_{sec}) or tertiary (k_{tert})) can be quantified using the experimental kinetic database available in the literature. Consequently, rate coefficients for the reactions of 33DMbutanal and 33DMbutanone with Cl atoms and OH and NO_3 radicals have been estimated with the SAR (Structure-Activity Relationship) predictive methods (Carter et al., 2021; Calvert et al., 2011; Jenkin et al., 2018; Kerdouci et al., 2014; Kwok and Atkinson, 1995). In the case of the two carbonyl compounds of this work, the only possibility of reacting is the abstraction of one hydrogen atom due to the absence of double bonds. The global abstraction rate coefficients can be calculated as $k_{\text{abs}} = 3(k_{\text{prim}}F(\text{C})) + k_{\text{sec}}F(\text{C})F(-\text{CHO}) + k_{\text{COH}}F(\text{CH}_2)$ for 33DMbutanal and $k_{\text{abs}} = 3(k_{\text{prim}}F(-\text{CR}_2\text{CO}-)) + (k_{\text{prim}}F(-\text{CO}-))$ for 33DMbutanone.

Con formato: Color de fuente: Rojo

Con formato: Fuente: Cursiva, Color de fuente: Rojo

Con formato: Fuente: Cursiva, Color de fuente: Rojo

Con formato: Fuente: Cursiva, Color de fuente: Rojo

Con formato: Color de fuente: Rojo

The rate coefficients (in $\text{cm}^3 \text{ molecule}^{-1} \text{ s}^{-1}$) and factors used to obtain the estimated rate coefficients for 33DMbutanal and 33DMbutanone with Cl atoms are: $k_{\text{prim}}=2.84 \times 10^{-11}$, $k_{\text{sec}}=8.95 \times 10^{-11}$, $k_{\text{COH}}=5.13 \times 10^{-11}$, $F(\text{C})=0.79$ proposed by Calvert et al., 2011, $F(-\text{CHO})=0.4$ proposed by Carter et al., 2021, $F(-\text{CR}_2\text{CO}-)=0.563$ and $F(-\text{CO})=0.037$ proposed by Farrugia et al., 2015. Therefore, the estimated rate coefficients for Cl reaction have been $k_{\text{estimated}} = 1.36 \times 10^{-10}$ and $k_{\text{estimated}} = 0.49 \times 10^{-10} \text{ cm}^3 \text{ molecule}^{-1} \text{ s}^{-1}$ for 33DMbutanal and 33DM-2-butanone respectively. In the case of OH reactions the rate coefficients have been estimated using the EPI (Estimation Programs Interface) Suite™, (US EPA), specifically the AOPWIN™. The rate coefficients estimated have been $k_{\text{estimated}}=2.212 \times 10^{-12}$ for 33DMbutanal and $k_{\text{estimated}}=1.69 \times 10^{-12}$ for 33DM-2-butanone. For the reaction of NO_3 radicals only the estimated rate coefficient for 33DMbutanal have been obtained $k_{\text{estimated}}=2.02 \times 10^{-14} \text{ cm}^3 \text{ molecule}^{-1} \text{ s}^{-1}$ using the data of Kerdouci et al., (2014). In all cases the estimated rate coefficients are very similar to the experimental values (see Table 1), indicating that the reactivity factors used for the estimations are well established. Reaction product studies and theoretical calculations of these reactions will help confirm the arguments presented above.

Con formato: Fuente: Cursiva, Color de fuente: Rojo

Con formato: Fuente: Cursiva, Color de fuente: Rojo

Con formato: Fuente: Cursiva, Color de fuente: Rojo

Con formato: Color de fuente: Rojo

Con formato: Fuente: Cursiva, Color de fuente: Rojo

Con formato: Fuente: Cursiva, Color de fuente: Rojo

Con formato: Color de fuente: Rojo

Con formato: Fuente: Cursiva, Color de fuente: Rojo

Con formato: Color de fuente: Rojo

Con formato: Fuente: Cursiva, Color de fuente: Rojo

Con formato: Color de fuente: Rojo

Con formato: Fuente: Cursiva, Color de fuente: Rojo

Con formato: Color de fuente: Rojo

3.2 Products study and Mechanisms of reaction

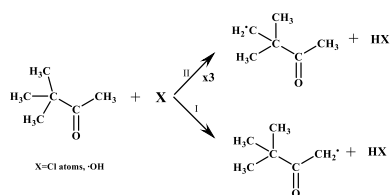
The products of the reactions of 33DMbutanal and 33DMbutanone with Cl atoms have been studied in the presence and in the absence of NO to evaluate different atmospheric conditions. In addition, the products of the reaction of 33DMbutanal with OH and NO_3 radical and 33DMbutanone with OH radicals have also been studied. All these reactions have been carried out using the experimental systems described above.

Con formato: Color de fuente: Rojo

The SAR method, explained above and used to estimate the rate coefficient, can also be used to define the branching ratios for hydrogen atom abstraction in the reaction of oxidant (Cl atoms, OH and NO₃ radicals) with a given saturated organic compound (Jenkin et al., 2018). In the Table 1S the percentages of hydrogen abstraction calculated for 33DMbutanone and 33DMbutanal are shown. For 33DMbutanone, the percentage of hydrogen abstraction from the -CH₃ group of the tert-butyl (channel II) is approximately 98% for Cl atoms and approximately 94% for OH radicals. These percentages are much higher than the percentages of hydrogen abstraction from the -CH₃ group in the α-position with respect to the carbonyl group (channel I) (~2% for Cl atoms and ~6 % for OH radicals). "x3" indicates three equivalent attack positions.

Based on the principles of tropospheric reactivity (Atkinson, 2007, Finlayson-Pitts and Pitts 2000) and in the case of 33DMbutanal in a previous products study with OH (Aschmann et al. 2010), a complete reaction mechanism has been proposed for both carbonyls to facilitate the identification of the products. The Scheme 1S and 2S (supplementary information) show these reaction mechanisms.

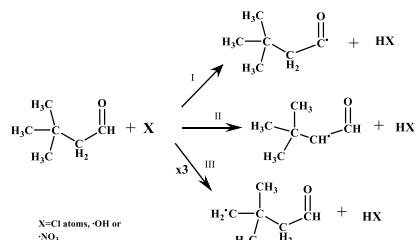
In the proposed mechanism for the reactions of 33DMbutanone (Scheme 1S), the initial attack by the oxidant can occur at the -CH₃ in the α position with respect to the carbonyl (channel I) or at any of the -CH₃ of the tert-butyl group (channel II).



For 33DMbutanal reactions, Aschmann et al. (2010) suggested that the primary pathway with OH radical involves hydrogen abstraction from the -CHO group (channel I). However, the SAR predictions indicate, that the main reaction channel varies with the oxidant type (see Table 1S). With Cl atoms, the major pathway is hydrogen abstraction from the -CH₃ group (~49%, channel III), followed by the -CHO group (~30%, channel I), and the -CH₂- group (~21%, channel II). For NO₃ radicals, the dominant pathway is hydrogen abstraction from the -CHO group (~63%, channel I), with the -CH₂- group (~37%, channel II) being the secondary channel. For OH radicals, the principal channel is hydrogen abstraction from the -CHO group (~94%, channel I), followed by the -CH₂- group (~4%, channel II), and -CH₃ group (~2%, channel III).

According to the SAR predictions the H-abstraction in the -CH₃ of the tert-butyl group is the main channel, for the reaction with both oxidants (~ 98 % for Cl atoms and ~ 94% for OH radicals, see Table 1S).

In the proposed mechanism of the reactions of 33DMbutanal (Scheme 2S), the initial attack can take place in three different groups: -CHO (channel I) -CH₂- (channel II) and -CH₃ (channel III) from tert-butyl group.



Aschmman et al., (2010) proposed the reaction in the -CHO group as the mayor initial channel of this compound with OH radicals. However, according to the SAR predictions used in this work, the main initial attack depends on the type of oxidants. Therefore, for the reaction with Cl atoms the main initial attack would take place in the -CH₃ (~49%) followed by -CHO (~30%) and lastly the -CH₂- group with ~21%. For the reaction of 33DMbutanal with NO₃ radical the main initial attack would take place in the CHO (~63%) followed by -CH₂- (~37%). And for OH reactions the main initial attack of the radical would take place in the -CHO (~94%) followed by -CH₂- (~4%) and lastly the -CH₃- (~2%). Note that the percentage of -CH₃ corresponds to three times the % of channel III (see Table 4S).

It is well established (Atkinson, 2007) that alkyl radicals, formed in the initial step of these reactions, rapidly react with O₂ to generate the corresponding peroxyradical (RO₂·). These RO₂ radicals can then follow various pathways (see Schemes 1S and 2S). In the absence of NO, peroxyradicals primarily undergo two self-reaction processes: one leading to the formation of alkoxyradicals (RO₂· + RO₂· → 2RO· + O₂), and the other producing two molecules neutral compounds, such as hydroxy compound and carbonyl compound (RO₂· + RO₂· → hydroxy compound + carbonyl compound + O₂). Another significant process is the reaction of RO₂ with OH radicals; and HO₂ radicals that undergoes different pathways (Bottorff et al., 2023; Berndt et al., 2022; Fittschen, 2019; Jenkin et al., 2019; Berndt et al., 2018; Winiberg et al., 2016), the likelihood of which depends on the size and structure of the alkyl group (R) (Berndt et al., 2018; Bottorff et al., 2023; Fittschen, 2019).

In the presence of NO, the RO₂ radical may react to form alkoxyradicals and NO₂ (RO₂· + NO· → RO· + NO₂) or nitrated compounds (RONO₂), and in presence of large concentration of NO₂, RO₂ generates peroxy-nitrated compounds (ROONO₂) (pathway less favoured). Under typical tropospheric conditions, alkoxyradicals can react with molecular oxygen (O₂), undergo unimolecular decomposition, or isomerize (Atkinson, 2007). The reaction of RO· radicals with O₂ is only possible if the carbon atom bearing the radical contains at least one hydrogen atom. Additionally, in the presence of NO and NO₂, alkoxyradicals can also form nitrated compounds (Atkinson, 2007).

~~In an effort to establish the main reaction paths for the reactions studied in this work, the rate coefficients for unimolecular decomposition and isomerization processes have been estimated in this work, using the method following the method outlined by Vereecken and Peeters (2009, 2010). In the case of 33DMbutanone, the rate coefficients for isomerization were much lower than those for decomposition making isomerization products insignificant. The estimated decomposition rate coefficient to form acetone ($1.7 \times 10^{12} \text{ s}^{-1}$) was much higher than to obtain butane-2,3-dione ($6 \times 10^3 \text{ s}^{-1}$). For 33DMbutanal the decomposition rate is four times higher than that for the isomerization process.~~

Con formato: Color de fuente: Rojo

estimated for the unimolecular isomerization of the initial alkoxyradical formed in both pathways were found to be at least one order of magnitude lower than the estimated rate coefficients for the decomposition of the same alkoxyradical. Consequently, the reaction products generated from isomerization channel will not be important. In channel II, the estimated rate coefficient of the decomposition process to obtain acetone has been $1.7 \times 10^{13} \text{ s}^{-1}$, that is much higher than the estimated rate coefficient to obtain butane-2,3-dione ($6 \times 10^3 \text{ s}^{-1}$). In the case of 33DMbutanal there is one possibility of isomerization in channel III where the H atom implied come from the aldehydic group. However, based on the estimated rate coefficients, the rate coefficient for decomposition is four times higher than that for the isomerization process.

Taking all the above into account, and to facilitate the qualitative analysis of reaction products from the reaction of 33DMbutanone and 33DMbutanal with atmospheric oxidants, proposed reaction mechanisms are depicted in Schemes 1S and 2S in the supplementary material. The $\text{RO}_2 + \text{HO}_2$ reactions are excluded to avoid further complicating the mechanism for 33DMbutanal, as they are significant only in the absence of NO_x , that is, in remote unpolluted atmospheres.

In the FTIR experiments, the residual IR spectra of the reaction products (obtained after subtracting the spectra of 33DMbutanone, 33DMbutanal, HCl , NO , NO_2 , CH_3NO_2 , N_2O_5 , HNO_3 , HNO_2 , etc.) were compared with IR spectra of commercial samples or database spectra (Eurochamp 2020 database <https://data.eurochamp.org/data-access/spectra/> last access: 9 July 2024). In those cases where quantification was possible, concentration-time plots were made to obtain information on whether the products formed are primary or secondary. Additionally, plots of product concentrations versus carbonyl consumption were created to determine the yields of the products formed from the slopes of these plots.

SPME/GC-TOFMS with EI and/or FI ionization was used as a qualitative technique to complement FTIR in identifying reaction products. The chromatograms collected at different reaction times, show peaks at different retention times whose areas increase with the reaction time, indicating that they correspond to reaction products. A specific software tool of the mass spectrometer was used to generate chromatograms (from the original chromatograms) with a lower signal to noise ratio to improve peaks visualization and thereby facilitating the analysis of the experiments performed using this technique. For that, in the software it is specified the desired m/z , or m/z range, and then the chromatogram is created (displaying the ion intensity versus time) with peaks representing the compounds that correspond to the specified m/z (or m/z range). In Fig. 2S a comparison of an original chromatogram and a chromatogram generated with this tool are shown. This tool has been used for all SPME/GC-TOFMS chromatograms obtained in EI mode. Due to the characteristic of SPME sampling method, only a qualitative analysis was possible. Mass spectra were analysed using the NIST database or compared with commercial samples. In some cases, a high similarity index allowed positive identification, but most assignments were tentative based on fragmentation patterns and proposed reaction products in schemes 1S and 2S. When FI spectra were available, the assignment was based on the m/z of the molecular ion fragment.

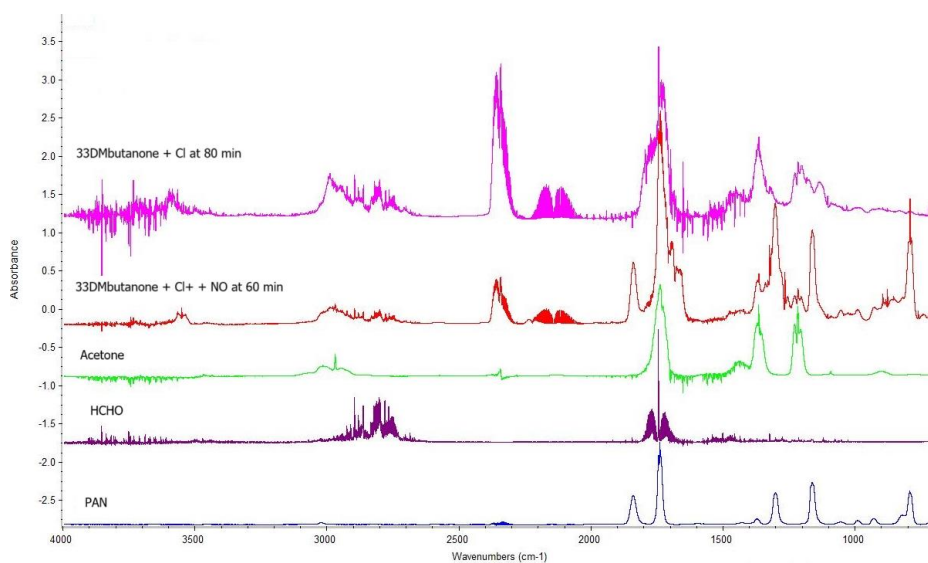
Next a discussion of the results on reaction products with both analytical techniques for each of the studied compound is presented. Based on the general mechanism proposed in Scheme 1S for 33DMbutanone and Scheme 2S for 33DMbutanal respectively, the formation of the expected products have been investigated using two analytical techniques. Also, the influence of the presence or absence of NO in the reaction of these two carbonyls with Cl atoms has been evaluated.

3.2.1 33DMbutanone

FTIR experiments

3.2.1 FTIR experiments

The identified and quantified reaction products were acetone ($\text{CH}_3\text{C}(\text{O})\text{CH}_3$) and formaldehyde (HCHO) for all reactions and nitrated compounds in those reactions carried out in the presence of NO and/or NO_2 . The nitrated compounds were attributed to alkoxy nitrates (RONO_2 , IR bands ~ 1663 , 1284 , 853 cm^{-1}) and peroxy nitrates (ROONO_2 , IR bands ~ 1720 , 1300 and 793 cm^{-1}) (Finlayson-Pitts and Pitts, 2000). A peroxy carbonyl nitrate such as PeroxyAcetyl Nitrate (PAN, $\text{CH}_3\text{C}(\text{O})\text{OONO}_2$, IR bands ~ 1830 , 1740 , 1300 and 793 cm^{-1}) was identified and quantified in the reactions of 33DMbutanone + Cl in the presence of NO after 3-5 minutes of reaction. Fig. 2 shows an example of residual spectra for the reactions of 33DMbutanone with Cl atoms in the absence and presence of NO. The figure includes reference spectra to confirm the formation of these compounds. Residual FTIR spectra for the reaction of 33DMbutanone with OH in the absence and presence of NO, are presented in Fig. 3S.



The procedure followed to analyse the FTIR spectra have been described in previous works (Aranda et al., 2020; Aranda et al., 2024; Colmenar et al., 2018, 2020a, 2020b). Therefore, only the main results will be indicated.

The residual IR spectra of the reaction products, obtained after subtracting the spectra of all known compounds (33DMbutanone, 33DMbutanal, HCl, NO, NO_2 , CH_3NO_2 , N_2O_5 , HNO_3 , HNO_2 , etc.), were compared with IR spectra of commercial samples or database spectra (Eurochamp 2020 database <https://data.eurochamp.org/data-access/spectra/> last access: 9 July 2024). The identified and quantified reaction products were acetone ($\text{CH}_3\text{C}(\text{O})\text{CH}_3$) and formaldehyde (HCHO) for all reactions (except to 33DMbutanal with NO_2); 2,2-dimethylpropanal ((22DMpropanal, $(\text{CH}_3)_3\text{CCHO}$)) for the reactions of 33DMbutanal with Cl atoms; and nitrated

compounds in those reactions carried out in presence of NO and/or NO₂. The nitrated compounds were attributed to alkoxy nitrates (RONO₂ ~1663, 1284, 853 cm⁻¹) and peroxy nitrates (ROONO₂ ~1718, 1300 and 793 cm⁻¹) (Finlayson-Pitts and Pitts, 2000). A peroxy carbonyl nitrates as PeroxyAcetyl Nitrate (PAN, CH₃C(O)OONO₂ ~1830, 1300 and 793 cm⁻¹) was identified and quantified in reactions of 33DMbutanone + Cl conducted in the presence of NO after 3-5 minutes of reaction time. Figure 2 shows an example of residual spectra from the reactions of 33DMbutanone and 33DMbutanal with Cl atoms in the absence and presence of NO. The figure includes reference spectra to corroborate the formation of these compounds.

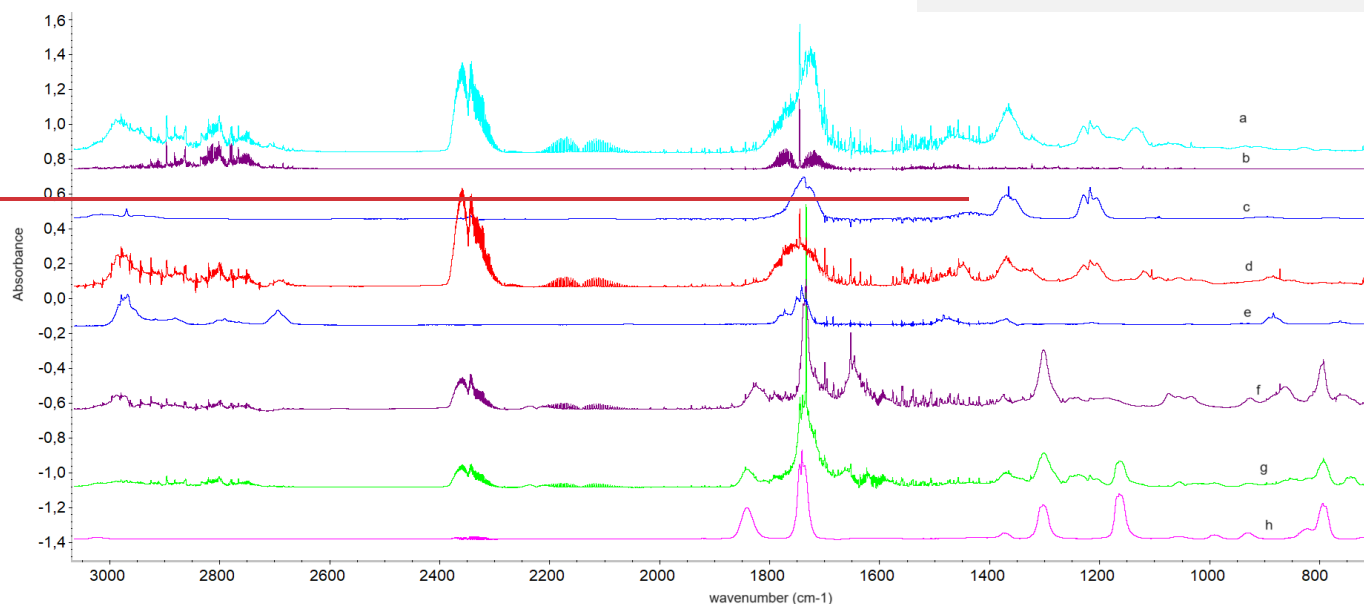


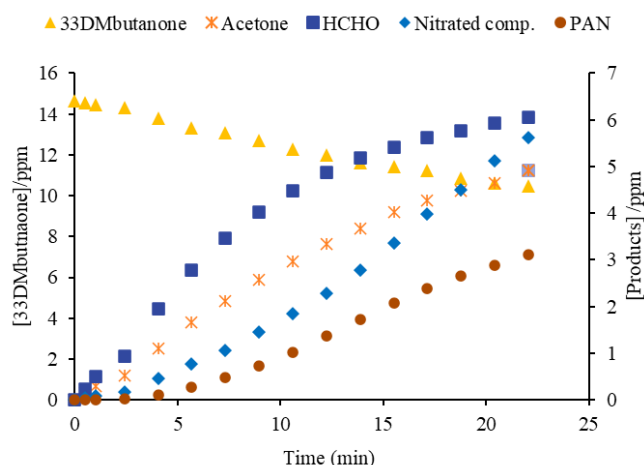
Figure 2. Residual FTIR spectra for the reactions of 33DMbutanone with Cl in the absence of NO (t=80 min) and in the presence of NO (t=60 min). Reference IR spectrum of HCHO, PAN (Eurochamp 2020 database <https://data.eurochamp.org/data-access/spectra/>) last access: 9 July 2024). Reference IR spectrum of acetone from a commercial sample. The spectra have been displaced for clarity.

After removing the IR absorption bands of formaldehyde and acetone from the spectra in Fig. 2, the newly obtained residual spectra reveal the presence of IR absorption bands characteristic of various organic functional groups, such as carbonyl (-C(O)- $\sim 1745\text{-}1795\text{ cm}^{-1}$) and hydroxyl ($\text{-OH, } \sim 3600\text{ cm}^{-1}$) (see Fig. 4S). As it can be seen, all the spectra show IR bands around $3725\text{-}3500\text{ cm}^{-1}$, $3000\text{-}2750\text{ cm}^{-1}$ and 1780 cm^{-1} , indicating the formation of common reaction products in the reactions of 33DMbutanone with Cl and OH. Other different IR bands (1136 , 1180 , 1364 cm^{-1}) are also identified, which would suggest different reaction products. Additionally, the IR bands shown in Fig. 4S are consistent with the multifunctional products proposed in Scheme 1S. Confirmation of these compounds is not possible due to their unavailability as commercial standards and the absence of reference spectra in existing infrared databases. Furthermore, the low intensity of their IR bands, likely resulting from low concentrations in the medium, combined with band overlap, hinders their identification.

To estimate the amount of nitrated compounds formed in the reactions with Cl atoms in the presence of NO, an average integrated absorption coefficient of $1.2 \times 10^{-17}\text{ cm molecule}^{-1}$ was used for the IR range $1250\text{-}1330\text{ cm}^{-1}$ based on similar compounds (Tuazon and Atkinson, 1990). For PAN quantification, the reference spectrum (Eurochamp 2020 database, <https://data.eurochamp.org/data-access/spectra/>) last access: September 2024) has been used. Fig. 3 shows the concentration-time profiles of the products and 33DMbutanone for the reactions with Cl in the presence of NO. Figure 2. Residual FTIR spectra for the reactions of: 33DMbutanone with Cl in the absence of NO at 21 min (a) and in the presence of NO at 21 min (g), 33DMbutanal with Cl atoms in the absence of NO at 18 min (d) and in the presence of NO at 18 min (f) 64 % of the conversion and a 29% respectively. Reference IR

Con formato: Interlineado: 1,5 líneas

spectrum of HCHO (b) acetone (c) (commercial sample), 22DMpropanal (e) and PAN (h). The spectra have been shifted for clarity.



Con formato: Centrado, Interlineado: Múltiple 1,15 lín.

For the reactions of 33DMbutanal with NO_3 , nitrated bands attributed to alkoxy nitrates, peroxy nitrates and peroxy carbonyl nitrates are clearly observed. The peroxy carbonyl nitrates could correspond to peroxy-3,3-dimethylbutyryl nitrate ($(\text{CH}_3)_2\text{CCH}_2\text{C}(\text{O})\text{OONO}_2$) that is formed due to the large amount of NO_2 presents in the reaction mixture from the initial time. Figure 3 shows the characteristic IR absorption bands of nitrated compounds formed in the reaction of 33DMbutanal with NO_3 .

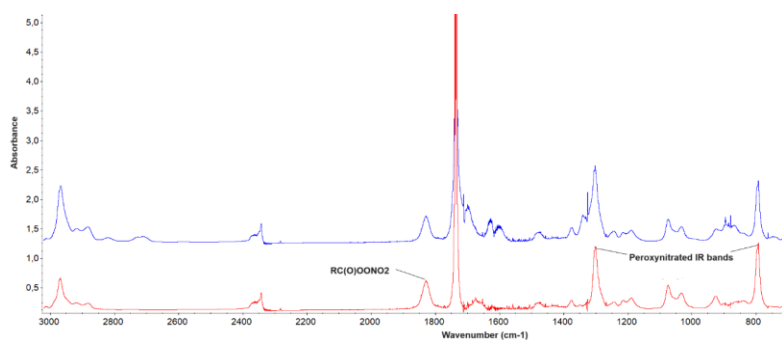


Figure 3. Concentration-time profiles of the products and 33DMbutanone for the reaction with Cl atoms in the presence of NO .

Figure 3. FTIR spectrum of the reaction of 33DMbutanal (~25% of conversion) with NO_3 radical (upper). FTIR residual spectra (assigned to peroxy-3,3-dimethylbutyryl nitrate) after elimination of N_2O_5 , HNO_3 , 33DMbutanal and NO_2 (lower).

The trend of the acetone and HCHO profiles indicate that they are primary products, although the concentration of HCHO starts to decrease after 20 min of reaction, possibly due to secondary chemical reactions such as photolysis or by the reaction with the main oxidant. The profile of the nitrated compounds, especially PAN, shows a significant increase after 5 minutes of reaction, related to the rise in NO_2 concentration in the medium after that time.

Fig. 4 shows an example of yield plots for the reactions of 33DMbutanone with Cl atoms in the presence of NO.

It is important to note that for the reactions of 33DMbutanal with Cl atoms (in the presence of NO) and with OH radical at large reaction times, a nitrated compound, as observed in the NO₂ reaction, has been detected. Additionally, IR bands of N₂O₅ (precursor of NO₃) has been observed in the reaction with Cl atoms as consequence of the reaction of O₃ + NO₂. This last result indicates the formation of ozone in the degradation process of 33DMbutanone/33DMbutanal in the presence of radiation and NO₂.

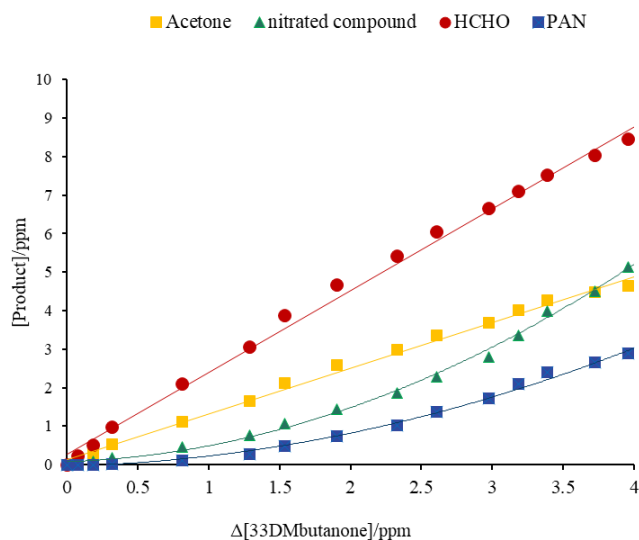


Figure 4. Plots of the reaction products formed versus the consumption 33DMbutanone in the reaction of Cl atoms in the presence of NO.

Figure 2S shows IR spectra of the nitrated compounds together with N₂O₅ reference spectrum. The IR bands of the nitrated compounds show great absorbance in the case of Cl reaction compared to the OH reactions. This fact could be due to an additional contribution from the 33DMbutanal reaction with NO₂. On the other hand, 22DMpropanal has not been observed in the reactions of 33DMbutanal with OH and NO₃ radicals, probably due to the overlapping of their characteristic IR bands with the ones of nitrated compounds.

The yields of nitrated compounds were estimated from the slopes of the plots showing linear behavior (using the initial data) to avoid contributions from secondary chemistry. For PAN, the data used were from a Δ[33DMbutanone] of approximately 2 ppm (see Fig. 5S). In the case of HCHO, the yield has been recalculated using the formalism published by Tuazon et al., 1986. The Fig.6S and Fig.7S of supplementary material show the concentration-time profiles and yield plots for the reactions of 33DMbutanone with Cl and OH in the absence of NO. The magnified residual spectra (see Fig. 8S) show IR absorption bands that can be assigned to formic acid. Formic acid is mainly produced through secondary reactions when formaldehyde is present, as evidenced by typical secondary concentration time profile (see Fig. 9S).

In the reaction of 33DMbutanone with Cl atoms and OH radicals in the presence of NO, the acetone yield is uncertain due to interference from the IR bands of the nitrated compounds. Additionally, the yields of HCHO and nitrated compounds in the reaction with OH radical were not determined due to contributions from other sources such as the precursor, methyl nitrite, and its degradation products (methyl nitrate and formaldehyde).

A summary of the estimated yields of reaction products, identified and quantified through FTIR analysis, is presented in Table 3. The yield of total carbon in % is calculated with Eq. (II)

$$Total\ carbon(\%) = \sum_i \frac{n^{\circ}\ of\ carbon\ of\ product_i}{n^{\circ}\ of\ carbon\ of\ carbonyl\ compound} \times molar\ yield_i \quad (II)$$

To evaluate the amount of nitrated compounds formed in the reactions studied with Cl atoms in the presence of NO, and in the 33DMbutanal reaction with NO₃ an estimation has been made using the average integrated absorption coefficient of 1.2×10^{-17} cm molecule⁻¹ corresponding to the IR range 1250-1330 cm⁻¹ for similar compounds (Tuazon and Atkinson, 1990). In the reaction of 33DMbutanal and 33DMbutanone with OH radicals, the yield of nitrated compounds was not estimated, because there is an additional contribution due to the precursor used (methylnitrite). For PAN quantification in the reaction of 33DMbutanone with Cl in the presence of NO, the reference spectrum (Eurochamp 2020 database, <https://data.eurochamp.org/data-access/spectra/>) last access: September 2024) has been used.

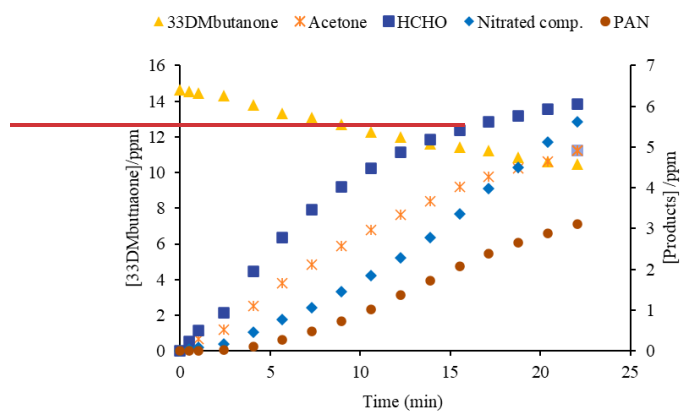
The time-concentration profiles of the quantified products formed, and the consumption of the carbonyl reactant have been represented in Figure 4.

Table 3. Estimated yields (%) and total carbon of reaction products identified with FTIR analysis, and the reaction products tentatively assigned from SPME/GC-TOFMS analysis in the reactions of 33DMbutanone with Cl atoms and OH radicals in the absence and presence of NO.

FTIR				
Reaction	Yield acetone (%) ± 2σ	Yield HCHO ^{a,b} (%) ± 2σ	Yield nitrated comp (%) ± 2σ	Yield PAN (%) ± 2σ
33DMbutanone + Cl	65.0 ± 1.1	153.3 ± 7.0	-	-
	65.9 ± 1.8	178.1 ± 4.1	-	-
	69.0 ± 1.3	174.7 ± 3.6	-	-
	Average	66.6 ± 4.2	168.7 ± 27.0	-
Total carbon (%)			61	
33DMbutanone + Cl + NO	123.2 ± 3.2	212.4 ± 7.4	59.2 ± 1.9	101.0 ± 7.0
	111.2 ± 6.3	195.4 ± 5.8	56.6 ± 6.6	112.9 ± 18.4
	137.4 ± 11.0	199.9 ± 11.5	66.9 ± 6.1	95.5 ± 11.0
	Average	124.0 ± 26.2	202.6 ± 17.6	202.6 ± 17.6
Total carbon ^c (%)			95.6	
33DMbutanone + OH ^d	31.4±2.0	59.5±2.4	-	-
	31.5±1.0	68.2±3.9	-	-
	34.1±1.6	73.5±4.2	-	-
	Average	32.3±3.0	67.0±14.0	-
Total carbon (%)			28	
33DMbutanone + OH + NO ^e	121.1 ± 6.7	-	-	-
	161.9 ± 19.7	-	-	-
	89.2 ± 6.4	-	-	-
	Average	93.0 ± 72.8	-	-
Total carbon (%)			47	
GC-TOFMS ^f				
Product (Retention time/min)	Cl	Cl + NO	OH + NO	
Acetone (2.2)	X	X	X	
Nitrated compound (2.6)			X	
Hydroxyacetone (2.9)	X			
Peroxyacetyl nitrate, PAN (5.6)		X		
4-Hydroxybutane-2,3-dione (7)	X	X		
22DM3oxobutanal (8.3)	X	X		
Nitrated compound (9.1)		X	X	
Nitrated compound (9.7)		X		
4H33DMbutanone (10.3)	X			
Nitrated compound (14.6)		X	X	

^aYields have been estimated using the reference IR spectra from the Eurochamp database (Rodenas et al., 2017). ^bThe rate coefficient used to correct the concentration of formaldehyde has been $k_{CF} = 7.2 \times 10^{-11} \text{ cm}^3 \text{ molecule}^{-1} \text{ s}^{-1}$ from IUPAC (2017). ^cNitrated compounds have not been accounted for total carbons. ^dOnly FTIR experiments using H₂O₂ as OH radical precursor. ^eExperiments using methyl nitrite as OH radical precursor. ^fThe positive identification and quantification were not possible due to the scarce of commercial samples. The quoted error in the individual yield (2σ) is two times the statistical errors from the regression analysis ($2 \times \sigma_{\text{slope}}$). The quoted error in the average yield (2σ) is two times the Standard deviation ($2 \times \sigma$). 22DM3oxobutanal (2,2-hydroxy-oxobutanal).

(a)



(b)

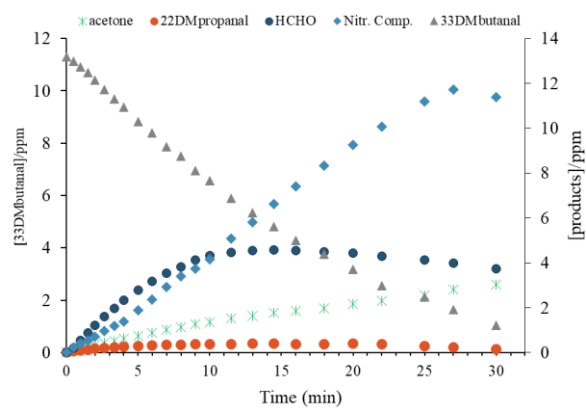


Figure 4. Time-concentration profiles of the products formed, and the carbonyl reacted for the reaction of (a) 33DMbutanone and (b) 33DMbutanal with Cl atoms in the presence of NO. For 33DMbutanone + Cl + NO, the nitrated compounds profiles are the total nitrated compounds (alcoxy, peroxy and PAN).

Table 3 shows that the total carbon recovery is less than 100%, however the residual FTIR spectra (Fig. 4S) indicate the formation of other reaction products not accounted for in the total carbon balance. In the reaction of 33DMbutanone with Cl atoms in the presence of NO the total carbon is 95% (without nitrated compounds yields). This high yield suggests possible overestimation of acetone and/or HCHO. In this regard, it should be noted that the calculated yields for acetone in reactions where nitrated compounds are generated have significant errors due to overlapping bands. On the other hand, as previously mentioned, the yields of the nitrated compound have been estimated using the average integrated absorption of similar compounds. Therefore, the yields of these nitrated compounds should also be interpreted with caution.

SPME/GC-TOFMS experiments

Fig. 5 shows an example of the SPME/GC-TOFMS chromatograms for the reactions of 33DMbutanone with Cl atoms and OH radicals. For the reaction with Cl atoms both EI and FI ionization modes were used. For the reaction with OH in the presence of NO, only the EI mode was used.

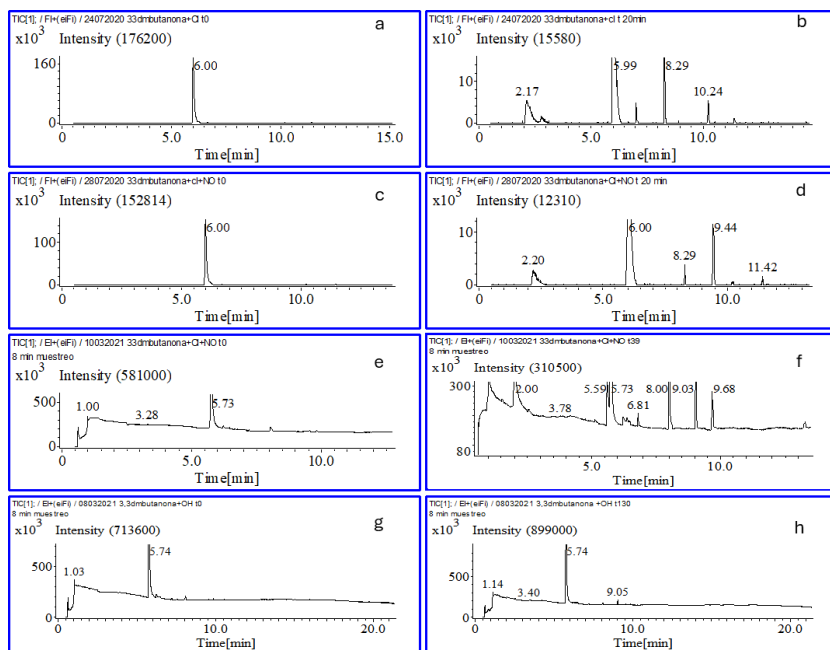


Figure 5. Example of the SPME/GC-TOFMS chromatograms for the reaction of 33DMbutanone + Cl atoms in the absence of NO and FI mode (reaction time t=0 min (a), t=20 min (b)) in the presence of NO and FI mode (reaction time t=0 min (c), t=20 min (d)) and in the presence of NO and EI mode (reaction time t=0 min (e), t=19 min (f)). Chromatograms (g) and (h) correspond to the reaction of 33DMbutanone + OH + NO at t=0 and t= 130 min of reaction respectively.

The FI chromatogram in the absence of NO (b) shows different peaks compared to that in the presence of NO (d), with two common peaks (t_r ~2.20 and ~8.3 min). This indicates that the presence of NO influences the reaction mechanism. In different ionization modes ((d) and (f) chromatograms), also result in a different number of peaks

suggesting some products were not ionized with FI (for example, peak at $t_r = 9.68$ min). Additionally, the peak of 33DMbutanone in chromatograms (e-h), appears at shorter retention times than in chromatograms (a-d), due to the use of a different chromatographic column. Taking into account this, the peaks at $t_r = 2.20, 6, 8.29$ and 9.44 min, showed in chromatograms (d) correspond to peaks at $t_r = 2.01, 5.73, 8.0$ and 9.03 min in chromatograms (f).

The SPME/GC-TOFMS chromatograms for the reaction of 33DMbutanone with Cl and with OH in the presence of NO (Fig. 10S) reveal both common peaks ($t_r \sim 2$ min, $t_r \sim 8$ min, $t_r \sim 9.0$ min and $t_r \sim 14.6$ min) and unique peaks for each reaction ($t_r \sim 2.5$ min for OH, and $t_r \sim 5.6$ min, $t_r \sim 6.8$ min and $t_r \sim 9.6$ min for Cl) which is consistent with the FTIR analyses. The mass spectra of all chromatographic peaks for the reaction products formed in the reactions with Cl atoms and with OH radicals in the presence of NO are shown in Table 2S. Due to the low intensity of chromatographic peak at $t_r = 8$ min for the OH reaction, it was not possible to obtain its mass spectrum with enough clarity.

The EI mass spectrum of each peak was analyzed using the NIST database of GC-MS. Except for acetone (98% of similarity index), the similarity index for the assignment of the reaction products was below 15%. This low similitude index may be due to low peak intensity (and thus the amount of product generated) or the absence of the mass spectra of the reaction products in the NIST database, either because the compounds are non-commercial or because they have not been previously reported in any bibliographic study. Without commercial samples, the formation of proposed products could not be confirmed, so only tentative assignments were made. These assignments were based on the m/z fragments of the mass spectra of these peaks, the expected m/z fragmentation pattern for the reaction products from Scheme 1S and the IR absorption bands from the residual spectra from FTIR experiments (Fig. 4S and Fig. 8S). In cases where the FI spectrum has been obtained, the assignment was also made based on the m/z fragment of the molecular ion.

In the Cl reaction without NO, the identification of a product with a molecular ion of $m/z = 116$ (at $t_r = 10.26$ min, see Table 2S) assigned to 4-hydroxy-3,3-dimethyl-2-butanone (4H33DM2butanone) is only explained by the self-reaction of two RO_2 radicals, leading to the formation of two molecules. In this case, the co-product molecule to 4H33DM2butanone would correspond to a compound with a molecular ion of $m/z = 114$ (at $t_r = 8.28$ min), assigned to 2,2-dimethyl-3-oxo-butanal (22DM3oxobutanal). This compound is also observed in the Cl reaction in the presence of NO, formed by the reaction of the alkoxy radical with O_2 . The peaks at $t_r = 2.55$ min with a $m/z = 72.08$ and the peak at $t_r = 7.03$ min with a molecular ion of $m/z = 102$ (see Table 2S) were assigned to hydroxyacetone and to hydroxybutan-2,3-dione respectively. The identification of these compounds indicates that the alkoxy radical also undergoes isomerization processes (see Scheme 3S).

The peaks only observed in the reactions with NO ($t_r = 5.59, 9.04, 9.68$, and 14.62 min for the Cl reaction, and $t_r = 2.55, 9.04$, and 14.62 min for the OH reaction) must correspond to the nitrated compounds (peroxy and/or alkoxy nitrates) proposed in scheme S1 and also observed in the residual spectra of the FTIR experiments (Fig. 2 and Fig. 3S). The analysis of the mass spectra for the peaks at $2.55, 9.04, 9.68$, and 14.62 min do not allow to identify clearly which nitrated compound they correspond to Scheme 1S. The peak at 5.59 minutes is identified as peroxyacetyl nitrate (PAN) which is unstable and decomposes in the injection port of the gas chromatograph. Upon decomposition, the $CH_3-C(O)OO$ radical could fragment generating the ions $CH_3-C(O)^+$ ($m/z = 43$) and $CH_3-C(O)O^+$ ($m/z = 59$). These fragments are like those observed in the EI mass spectrum (see Table 2S). There is not any reference mass spectrum to compare, only two studies determined the chemical ionization mass spectrum of PAN (Phillips et al., 2013; Pate

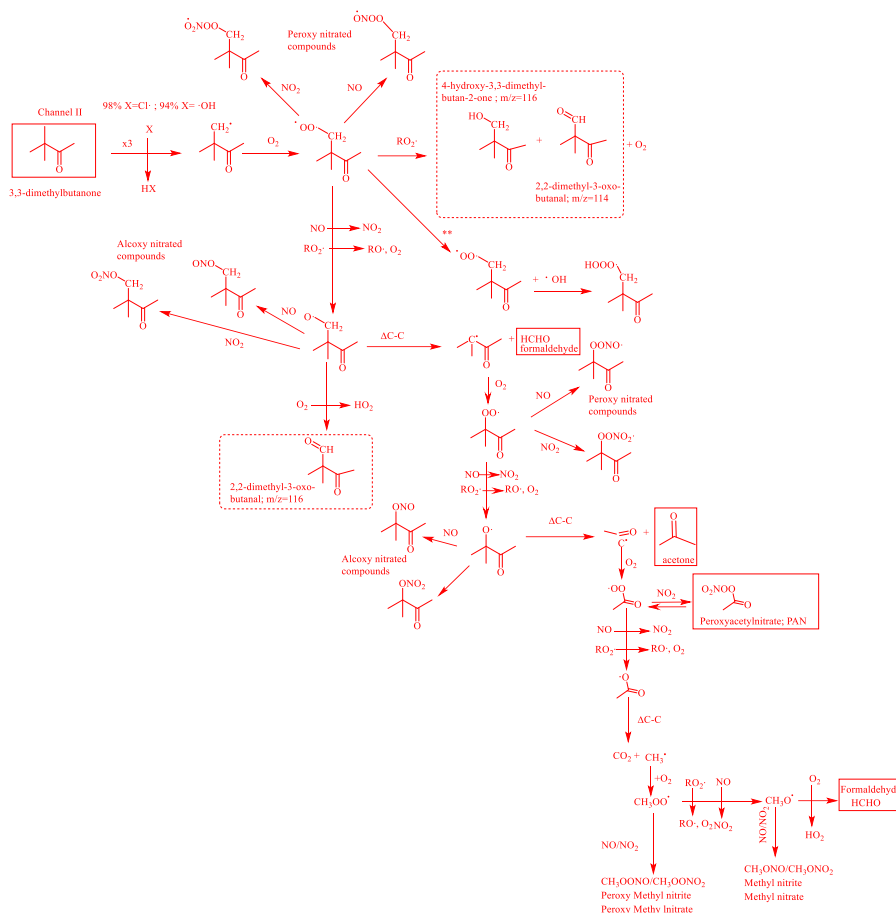
et. al., 1976). Moreover, considering that PAN is clearly detected in the experiments conducted with the FTIR system and that the mass spectrum corresponding to the chromatographic peak with a retention time of $t_r = 5.59$ min does not account for the formation of any other compound proposed in Scheme 1S, it was concluded that this peak likely corresponds to PAN.

The main reaction products tentatively assigned from SPME/GC-TOFMS analysis are shown in Table 3. The SPME/GC-TOFMS experiments confirm the formation of acetone as identified and quantified in the FTIR experiments. However, formaldehyde was undetectable due to the SPME sampling method. Other proposed products include various multifunctional organic compounds (Hydroxybutan-2,3-dione, 2,2DM3oxobutanal, 4H33DM2butanone) and nitrated compounds with different carbon chain lengths.

Table 3 shows that the percentage of acetone and formaldehyde is higher in reactions with Cl and OH in the presence of NO compared to those without NO. This indicates that NO favors the formation of the alkoxy radical by reaction of the peroxy radical that is chemically activated and undergo prompt decomposition to form acetone (Atkinson, 2007). In the absence of NO, the percentage of acetone is lower in the OH reaction than in the Cl reaction, possibly due to the formation of other products such as RO₂OH by the reaction of RO₂ with OH radical (Berndt et al., 2022; Fittschen, 2019; Jenkin et al., 2019). This compound could not be identified due to the lack of a reference IR/MS spectrum. The IR bands at 3700-3500 cm⁻¹ in the residual spectrum of 33DMbutanone with OH in the absence of NO may be due to the OH stretching vibration in the ROO-OH molecule. The IR band at ~1800 cm⁻¹ for 33DMbutanone + Cl reaction (Fig. 2 and Fig. 4S) could correspond to the stretching vibration of the C=O (carbonyl bond) in the acyl chloride. This compound can be formed by the reaction of RO₂ with Cl₂ or Cl atoms (Ren et al. 2018).

Considering that the formation of PAN can only be explained via channel II (hydrogen abstraction from the -CH₃ group of the tert-butyl group), which involves the decomposition of the initially formed alkoxy radical (2,2-dimethyl-3-oxobutan-1-yloxy radical), and that the plot of PAN concentration versus the variation in 33DMbutanone concentration shows a linear relationship with a slope close to one (indicating an estimated PAN yield of 100%, see Fig. 5S), it could be concluded that the percentage of Cl attack on the -CH₃ group of the tert-butyl group is nearly 100%. This value closely with the 98% estimated by the SAR method for reactions with Cl (see Table 1S). For reactions with OH, only acetone and HCHO were quantified but with the obtained yields do not confirm that 94% of the reaction proceeds through channel II, as suggested by the SAR. However, considering that the rate coefficient estimated by the SAR method is similar to the experimental one, channel II can be considered the main process.

Finally based on the kinetic results and the products observed in this study, the reaction mechanism for the degradation of 33DMbutanone is shown in Fig. 6.



616

617 **Figure 6. Mechanism proposed for the formation of the reaction products observed for 3,3-dimethylbutanone reactions**
 618 **with Cl atoms and OH radicals. The solid framed products correspond to products quantified by FTIR and dotted**
 619 **framed correspond to product identified by SPME/GC-TOFMS. x3 indicates that there are 3 equivalent attack**
 620 **positions. ** pathway proposed to reaction of 3,3-dimethylbutanone with OH in the absence of NO.**

621 3.2.2 3,3-dimethylbutanal reaction

622 FTIR experiments

623 Fig. 11S shows an example of the residual IR spectra of the reaction of 3,3-dimethylbutanal with Cl atoms (in the absence
 624 and presence of NO), OH radicals and NO₃ radicals (obtained after subtracting the spectra of all known compounds).
 625 The reaction products identified and quantified from these residual spectra were: acetone, HCHO and 2,2-
 626 dimethylpropanal ((2,2DMpropanal, (CH₃)₃CCHO)) for the reactions with Cl atoms, acetone for the reactions with
 627 OH radicals and nitrated compounds for the reaction with NO₃ radicals.

The IR bands of peroxy carbonyl nitrates observed in the residual spectra of NO_3 reactions (~ 1830 , 1710 , 1300 and 790 cm^{-1}) could correspond to peroxy-3,3-dimethylbutyryl nitrate ($(\text{CH}_3)_3\text{CCH}_2\text{C}(\text{O})\text{OONO}_2$) that is formed due to the large amount of NO_2 presents in the reaction mixture from the initial time. Fig. 7 shows the characteristic IR absorption bands of nitrated compounds formed in the reaction of 33DMbutanal with NO_3 .

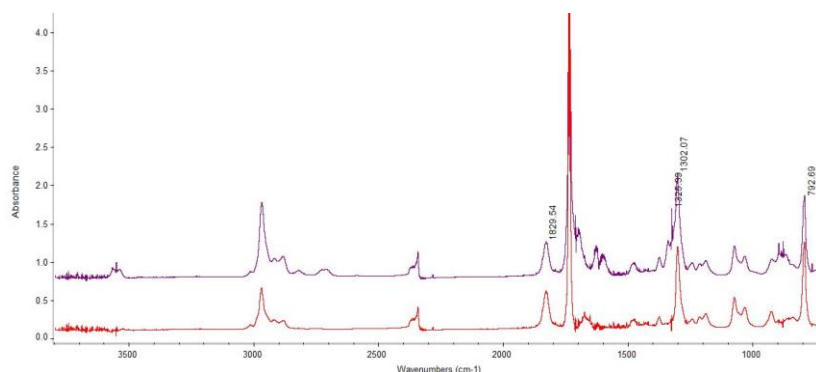


Figure 7. FTIR spectrum of the reaction of 33DMbutanal (at 21 min) with NO_3 radical (upper). Residual FTIR spectrum (assigned to peroxy-3,3-dimethylbutyryl nitrate) after elimination of N_2O_5 , HNO_3 , 33DMbutanal and NO_2 (lower).

In the reactions of 33DMbutanal with Cl atoms in the presence of NO and with the OH radicals at long reaction times, IR bands corresponding to a nitrated compound (similar to the one in the reaction with NO_3) have been detected. IR bands of N_2O_5 (a precursor of NO_3) have also been observed in the reaction with Cl atoms in the presence of NO as a consequence of the reaction between O_3 and NO_2 (see Fig. 12S). This indicates the formation of ozone in the degradation process of 33DMbutanal with Cl atoms in the presence of NO at long reaction times. The IR bands of the nitrated compounds show greater absorbance in the case of Cl reactions compared to the OH reactions, possibly due to an additional contribution from the 33DMbutanal reactions with NO_3 . On the other hand, 22DMpropanal has not been observed in the reactions of 33DMbutanal with OH and NO_3 radicals, likely due to the low concentration of this compound and the overlap of its characteristic IR bands with those of nitrated compounds.

After removing the IR absorption bands of the identified products in Fig. 11S, the residual spectra reveal the presence of IR absorption bands characteristic of carbonyl (~ 1700 - 1790 cm^{-1}), hydroxyl (~ 3600 and 1033 cm^{-1}) and organic acid/acetyl chloride compound ($\sim 1800\text{ cm}^{-1}$) (Fig. 12S). The amplified residual spectra of Fig. 12S (Fig. 13S) shows clearly some IR absorption bands that appear at the same wavenumber indicating common reaction products. The IR band at 1105 cm^{-1} shown in Fig. 13S again indicates the formation of formic acid.

The trends of the concentration-time profiles of the quantified products for the reaction of 33DMbutanal with Cl atoms (Fig. 14S), suggest that they are primary products in the early stages (linear trend). However, it is observed that after a certain reaction time, the concentrations of 22DMpropanal and HCHO decrease. This decrease could be attributed to loss processes involving reactions with Cl atoms and/or photolysis. Additionally, the concentrations of acetone and nitrated compounds are observed to increase more than expected (profile with an upward trend, Fig. 14Sb), likely due to contributions from secondary chemistry, such as the previously discussed reactions, of 22DMpropanal with Cl or its photolysis. For the nitrated compounds, a change in the trend is observed around 2

minutes likely due to the formation of nitrated peroxy carbonyl compounds because of the presence of large amounts of NO₂ in the reaction mixture. The profile of nitrated compounds from the reaction of 33DMbutanal with NO₂ (Fig. 14Sd), shows an increase from the start of the reaction, attributed to the presence of NO₂ in the reaction medium from the beginning.

The concentration plots of the products formed against the variation 33DMbutanal, used to obtain the yields, are shown in Fig. 15S. For of HCHO and 22DMpropanal, where the concentration decreases by react with the main oxidant, the yield has been recalculated using the formalism by Tuazon et al. 1986. In the reaction of 33DMbutanal with the OH radical, the yield of HCHO and nitrated compounds has not been determined for the same reason as in the 33DMbutanone reactions. A summary of the estimated yields of reaction products, identified and quantified through FTIR analysis is presented in Table 4 for the reaction of 33DMbutanal with the three oxidants.

SPME/GC-TOFMS experiments

The SPME/GC-TOFMS chromatograms in EI mode show peaks at different retention times that increase with reaction time (see Fig. 16S), indicating that they correspond to reaction products. The number of significant peaks is higher in the reaction of 33DMbutanal with Cl atoms and NO₃ radicals compared to the reaction with OH radicals, where only 3 peaks are observed (see Fig. 17S-20S). This difference is likely due to the different attack positions (channels) of the oxidant: 3 for Cl atoms, 2 for NO₃ radicals, and 1 for OH radicals, as estimated by the SAR method (see Table 1S). Some of these peaks have similar retention times and mass spectra (see Table 3S), indicating that they are the same products. Some of these products are also identified in the FTIR analysis (see Table 4) such as acetone (*t_r* = 2.2 min) and 22DMpropanal (*t_r* = 3.08/3.43 min, confirmation with the injection of a real sample of 22DMpropanal).

It is interesting to note the presence of a common peak for all reactions that appears at 9.56 min (8.95 min in the experiment with a new chromatographic column). The mass spectrum of this peak is assigned to 3,3-dimethylbutanoic acid (33DMbutanoic acid) by the NIST database software, with a similarity index of approximately 87%. The formation of this compound cannot be explained by the general scheme proposed (Scheme 2S), which is based on principles of atmospheric reactivity and bibliographic studies of similar compounds (Aschmann et al., 2010; Atkinson, 2007). To explain the formation of this peak, other pathway was initially proposed, where the oxy-3,3-dimethylbutyryl radical (channel I), undergoes isomerization (see Scheme S4). This pathway leads to the formation of 4-oxo-3,3-dimethylbutanoic acid, whose mass spectrum shows a fragmentation pattern very similar to the peak with a *t_r* of 9.56 min. Taking into account that 33DMbutanoic acid is a commercial compound, a sample was injected into the SPME/GC-TOFMS system. The chromatogram showed a peak at approximately 9 minutes, with a mass spectrum (see Fig. 21S) identical to that of the peaks (9.56/8.95 min, see Table 3S) which positively confirms the formation of 33DMbutanoic acid in the reactions of 33DMbutanal with Cl atoms and OH and NO₃ radicals. The characteristic IR bands of 33DMbutanoic acid seem to be present in the residual FTIR spectra obtained for the reaction of 33DMbutanal with Cl atoms (Fig. 22S). Recent studies have also detected organic acids from reactions of saturated aldehydes (Asensio et al., 2022; Bo et al., 2022).

The remaining chromatographic peaks shown in Fig.17S-20S, have been assigned to reaction products depicted in Scheme 2S (except the peaks at 16.2 and 21 min). Table 3S contains the mass spectra and their product assignments. In general, the complete interpretation of mass spectra is complex due to the similar structures of the products formed, leading to similar fragmentation patterns. The EI mass spectrum of each peak was analyzed using the NIST

database of GC-MS. The similitude index for most reaction products is low except for acetone (98%) and of peak at 5.47 min in the NO₃ reaction, assigned to 2,2-dimethylpropanol (22DMpropanol) with a similarity index of 73.5%. The mass spectrum of peaks around 8 min (7.88, 8.23 and 8.26 min) could correspond to several structurally similar products for example, 2,2-dimethyl-butanodial (22DMbutanodial), 3,3-dimethyl-oxobutanal (33DMObutanal) and 2,2-dimethylpropanoic acid (22DMpropanoic acid). A commercial sample of 22DMpropanoic acid injected into the SPME/GC-TOFMS system showed a chromatogram with a peak at 8 minutes, matching the mass spectrum of the peak at 8.23 min observed in the reaction of 33DMbutanal with Cl atoms with NO. Fig. 22S, shows an IR reference spectrum of 22DMpropanoic acid. 22DMbutanodial and 33DMObutanal could not be positively confirmed due to the lack of commercial samples.

As can be seen in Table 3S, some of the proposed reaction products are dicarbonyl and/or hydroxycarbonyl compounds with IR bands also present in the residual spectra (Fig. 12S and Fig. 13S). Hydroxycarbonyl compounds tend to cyclize to dihydrofurans via acid-catalyzed heterogeneous reactions (Atkinson et al., 2008). For example, 4-hydroxy-3,3-dimethylbutanal (4H33DMbutanal, t_r = 15.78 min) can cyclize to form 2,3-dihydro-4,4-dimethylfuran (23DH44DMfuran). Another cyclization process can occur from an alkoxy carbonyl radical, such as the 4-formyl-2,2-dimethylbutan-1-yloxy radical, leading to the formation of 2,2-dimethyltetrahydrofuran-2-one (22DMTHfuranone, t_r = 13.25 min). A similar cyclization could explain the formation of 3,4-dimethyldihydrofuran-2,3-dione (34DMDHfuran23dione, t_r = 16.2 min) observed in the reaction with Cl atoms and assigned by the NIST database with a similarity index of 62%. The peak at 6.97/6.86 min, observed in the Cl + NO and NO₃ reactions, has been assigned to a nitrated compound, possibly peroxy-3,3-dimethylbutyryl nitrate also detected in the FTIR analysis. The intensity of this peak is low, likely due to thermal decomposition in the chromatograph injector. Another small peak at 7.15 min, observed in the NO₃ and OH radical reactions, could correspond to peroxy nitrite (in the case of the OH reaction) and peroxy nitrate (for the NO₃ reaction), based on IR bands of peroxy compounds at 793 cm⁻¹ observed in the FTIR spectra (see Fig. 13S). Fig. 13S also shows an IR band at 810 cm⁻¹ for the Cl + NO and OH reactions, characteristic of alkoxy nitrated compounds. This common product was not detected in SPME/GC-TOFMS, possibly due to adsorption onto the fiber. Generally, SPME/GC-TOFMS is not effective for sampling for nitrated compounds.

The products assigned in the qualitative analysis of the SPME/GC-TOFMS experiments, along with the products identified and quantified using FTIR are shown in Table 4. The total carbon yield in % is calculated with Eq. (II).

Table 4. Estimated yields and total carbon (%) for reaction products formed in the reactions of 33DMbutanal with the atmospheric oxidants using FTIR and the products identified in the qualitative analysis using GC-TOFMS.

Reaction	FTIR			
	Yield 22DMpropanal ^{a,b} (%)±2σ	Yield Acetone (%)±2σ	Yield HCHO ^{b,c} (%)±2σ	Yield Nitrated comp. (%)±2σ
33DMbutanal + Cl	28.4±0.4	31.1±0.6	37.4±0.6	-
	29.6±0.3	26.8±0.4	38.5±0.7	-
	29.9±2.0	27.5±0.3	40.5±2.1	-
Average	29.3±1.4	28.5±4.8	38.8±3.1	-
Total carbon (%)	45			
33DMbutanal + Cl + NO	7.1±0.5	20.3±0.6	83.3±3.8	52.1±3.1
	7.1±0.2	20.8±0.3	89.2±2.3	50.3±3.2

	6.7±0.2	22.4±1.0	95.3±6.2	52.5±2.0
Average	7.0±0.4	21.1±2.1	89.3±12.0	51.6±2.3
Total carbon^d (%)	31			
33DMbutanal + OH + NO	Not observed	24.9±0.8	-	-
		34.6±1.0	-	-
		37.1±0.7	-	-
Average		32.2±13.0	-	-
Total carbon (%)	16			
				102±2.3
33DMbutanal + NO₃	Not observed	Not observed	Not observed	105±1.0
				108±1.0
				107±1.0
Average				106±5.0
GC-TOFMS^c				
Product (Retention time/min)	Cl	Cl + NO	OH + NO	NO₃
Acetone (2.2)	X	X	X	X
Hydroxyacetone (2.7)	X			
22DMpropanal (3.4)	X	X		X
22DMpropanol (5.8)	X	X		X
Peroxy-3,3-dimethylbutyryl nitrate (7)		X		X
Peroxy nitrated compound (7.2)			X	X
22DMbutanodial/33DMObutanal/				
22DMpropanoic acid (8-8.2)	X	X		X
33DMbutanoic acid (9.6)	X	X	X	X
22DMTHfuran-2-one (13.3)	X	X		
4H33DMbutanal/	X			
(23DH44DMfuran (15.8)	X			

^aThe rate coefficient used to correct the concentration of 22DMpropanal has been $k_{Cl}=1.42\times10^{-10}$ cm³ molecule⁻¹ s⁻¹ from Calvert et al., (2011). ^bYields have been estimated using the reference IR spectra from the Eurochamp database (Rodenias et al., 2017). ^cThe rate coefficient used to correct the concentration of formaldehyde has been $k_{Cl}=7.2\times10^{-11}$ cm³ molecule⁻¹ s⁻¹ from IUPAC (2017). ^dNitrated compounds have not been accounted for. ^eThe positive identification and quantification were not possible to scarce of commercial compounds. Only 22DMpropanal; 33DMbutanoic acid and 33DMbutanoic acid were confirmed with a commercial sample. The quoted error in the individual yield (2σ) is two times the statistical errors from the regression analysis ($2 \times \sigma_{slope}$). The quoted error in the average yield (2σ) is two times the Standard deviation ($2 \times \sigma$).

The analysis of these quantified compounds provides insights into the percentage of each reaction channel or favored pathway. Acetone is a reaction product formed from all channels (see Scheme 2S). According to Aschmann et al. (2010) about reaction of 33DMbutanone with the OH radical the percentage of channel I is 94%, with acetone, tert-butyl nitrite and tert-butyl nitrate as the main reaction products. Therefore, considering the results of Aschmann et al. (2010), the acetone quantifies in our work for the reaction of 33DMbutanone with OH (32%) would be formed mainly through channel I. In the reaction with Cl without NO, the acetone yield (28%) is close to the percentage predicted by the SAR method for channel I (30%). HCHO is also formed through all three channels. However, the highest yield of formaldehyde, along with the significant decrease of 22DMpropanal obtained in the reaction of Cl + NO compared to the yields of Cl reaction without NO, suggest that, in the presence of NO, the reaction of the peroxy species generated in channel I or channel II to form nitrated compounds is favored over the expense of the self-reaction of RO₂.

The total carbon calculated for the Cl reaction in the absence of NO, based on the yields of HCHO, acetone, and 22DMpropanal, accounts for only 45%. The remaining carbon can be explained by the formation of other

compounds identified through SPME/GC-TOFMS. Lower yields in the Cl reaction with NO (33%) and OH (16%) could be attributed to the significant formation of nitrated compounds, not included in the total carbon calculation. For the NO₃ radical reaction, the linear trend observed in Fig. 15S (d) indicates that 100% of the reacted 33DMbutanal forms nitrated compounds. If only peroxy-3,3-dimethylbutyl nitrate was generated, the total carbon would be 100%, indicating that no other compounds were formed in the reactions with NO₃. However, as in the case of reactions with 33DMbutanone, the yield of nitrated compounds should be considered with caution. The identification of other compounds in the SPME/GC-TOFMS analysis could be due to the rapid decomposition of peroxy-nitrated compounds in the injection port or overestimation of nitrated compound yields. Quantification is necessary to determine if these products are generated in significant amounts, but this is not possible due to the lack of commercial compounds or the characteristics of the SPME sampling method.

No exclusive compounds for each reaction channel (I, II, or III) have been quantified for the 33DMbutanal reaction, making it impossible to determine the percentage of each channel. The formation of 33DMbutanoic acid in all reactions suggest another reaction pathway not considered in Scheme 2S, as RO₂ + HO₂ reactions are less likely in the presence of NO/NO₂. A proposed reaction pathway explains the formation of the 33DMbutanoic acid:



The IR bands of ozone are not observed in the residual spectra of Fig. 13S, likely due to the low amount of O₃ and overlapping IR bands. A similar reaction was proposed for the CH₃C(O)OO radical by other authors (Groß et al., 2014; Dillon and Crowley, 2008; Tomas et al., 2001). On the other hand, 22DMpropanoic acid (observed in the 33DMbutanal with Cl atoms) could be a secondary product from the degradation of 22DMpropanal. The yields of organic acids from the corresponding aldehyde must be very low (Bo et al., 2022), making pathway (R9) a minority reaction.

Based on the discussion about the reaction products done above, previous studies of 33DMbutanal with the OH radical (Aschmann et al., 2010) and estimated percentages for each channel using the SAR method, the scheme 2S initially proposed by the reaction mechanism for 33DMbutanal with Cl atoms, OH and NO₃ radicals has been simplified in Fig. 8.

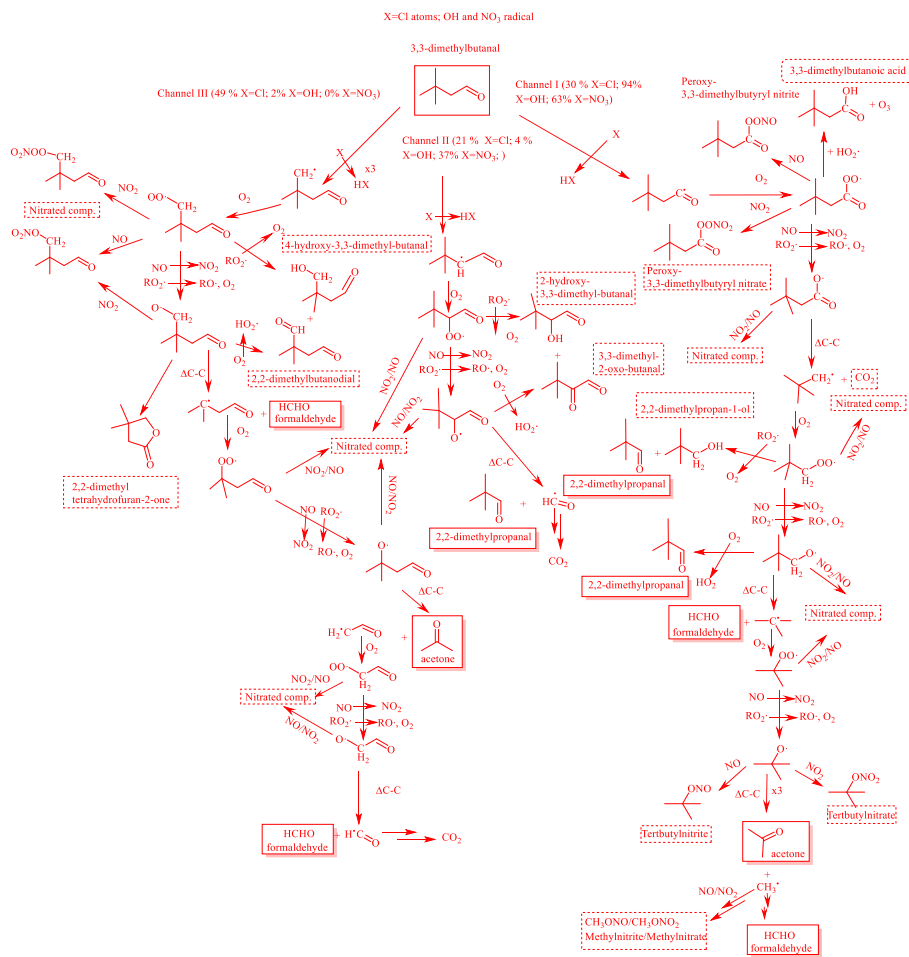


Figure 8: Mechanism proposed by the formation of the main reaction products observed for 33DMbutanal reaction with Cl atoms, OH and NO_3 radical. The solid framed products correspond to products quantified by FTIR and dotted framed products correspond to identified by SPME/GC-TOFMS.

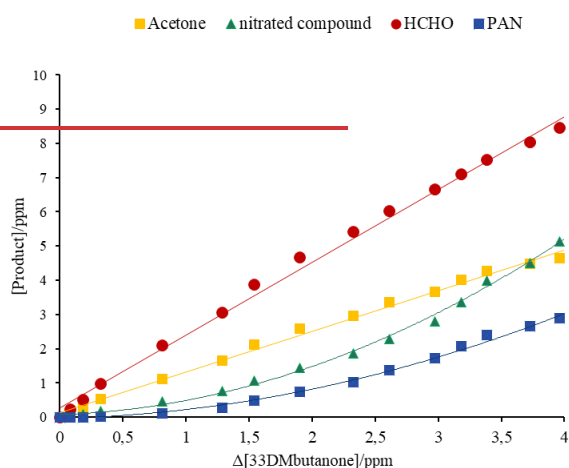
For the reaction of 33DMbutanal with Cl atoms, the trends of acetone and HCHO indicate that they are primary products, although the concentration of HCHO starts to decrease at 20 min of reaction, possibly due to secondary chemical reactions. The profile of nitrated compounds, especially PAN, shows a significant increase after 5 minutes of reaction. In the case of the reaction of 33DMbutanal with Cl atoms, all trends (for acetone, HCHO, 22DMpropanal and nitrated compounds) suggest that they are primary products in the early stages. However, 22DMpropanal and HCHO seem to undergo further reactions due to secondary chemistry, while the concentrations of acetone and nitrated compounds increase more than expected, likely due to contributions from other sources (Figures 3S–5S). For the nitrated compounds, a change in the trend is observed around 2 minutes, likely due to the formation of nitrated peroxy carbonyl compounds as a result of the presence of NO_2 in the reaction mixture. The

Con formato: Interlineado: 1,5 líneas

profile of nitrated compounds from the reaction of 33DMbutanal with NO₃ shows an increase from the initial of the reaction (see Figure 4S), due to the presence of NO₂ in the reaction medium from the beginning.

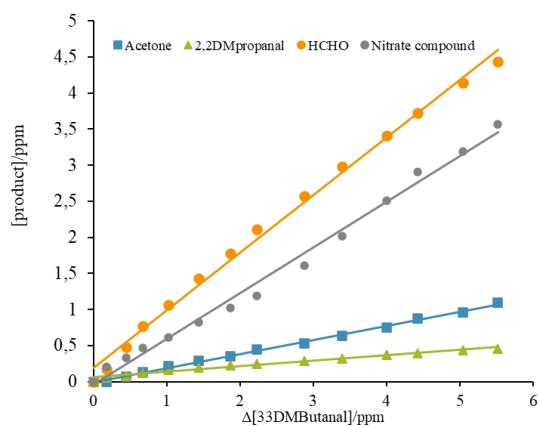
The yields for primary products have been calculated from the slopes of the plots of the concentration of the products formed against the variation in the carbonyl reactant consumed using the first data of the reactions to avoid secondary chemistry contributions. In some cases, the yields have been difficult to obtain due to the overlapping of IR bands with other unidentified products. In these cases, in which the concentration of the compounds that seems to react with the main oxidant (such as 22DMpropanal and HCHO) the yields have been recalculated using the formalism published by Tuazon et al., 1986. Figure 5 showed an example of yield plots for the reactions of 33DMbutanal with Cl atoms in the absence and the presence of NO. The yield of PAN formed in the reaction of 33DMbutanone with Cl atoms in the presence of NO has been estimated from the slopes of the plots, where the data show a linear behavior, corresponding to a $\Delta[3,3\text{DMbutanone}]$ of approximately 1.5 ppm (see Figure 5a).

796 (a)



797

798 (b)



799

800 Figure 5. Plots of the reaction product formed versus the consumption of the reactant in the reaction of (a)
801 33DMbutanone + Cl + NO and (b) 33DMbutanal + Cl + NO.

802 The Figures 6S and 7S of supplementary material show the yield-plots for the reactions of 33DMbutanone and
803 33DMbutanal with Cl atoms and 33DMbutanone with OH in the absence of NO respectively.

804 A summary of the estimated yields of reaction products, identified and quantified through FTIR analysis, is presented
805 in Table 3 for the reaction of 33DMbutanone + Cl, Cl + NO and + OH radical. Table 4 shows the results for the
806 reactions of 33DMbutanal + Cl; Cl + NO, OH and NO₂ radical.

1 Table 3. Estimated yields (%) of reaction products identified with FTIR analysis and the reaction products tentatively assigned from SPME/GC-TOFMS analysis in the reactions
 2 of 33DMbutanone with Cl atoms and OH radical in the absence and in the presence of NO.

Reaction	FTIR				GC-TOFMS	
	Yield acetone (%)±2σ	Yield HCHO ^{a,b} (%)±2σ	Yield nitrated comp. (%)±2σ	Yield PAN (%)±2σ	tr minutes	Reaction Product
33DMbutanone + Cl	65.0±1.1	153.3±7.0			2.2	Acetone
	65.9±1.8	178.1±4.1			2.87	Hydroxyacetone
	69.0±1.3	174.7±3.6			7.03	Hydroxy 2,3 butanodione
	Average	66.6±4.2	168.7±30.0		8.28	2,2DM3-oxo-butanal
Total carbon^{c,d} (%)		61			10.26	4 hydroxy 3,3 DM2butanone
33DMbutanone + Cl + NO ^e	123.2±3.2	212.4±7.4	59.2±1.9	101.0±7.0	2 ^g	Acetone
	111.2±6.3	195.4±5.8	56.6±6.6	112.9±18.4	5.59	Peroxyacetyl nitrate (PAN)
	137.4±11.0	199.9±11.5	66.9±6.1	95.5±44.2	6.81*(7.03) ⁽⁺⁾	Hydroxy 2,3 butanodione
	Average	124.0±26.2	202.6±17.6	103.1±8.8	8.01*(8.28)	2,2DM3-oxo-butanal
					9.04	2,2 dimethyl 3-propyl-oxynitrite
					9.68	Nitrated compound
Total carbon^{c,d} (%)		95.6			14.57	Nitrated compound
33DMbutanone + OH ^a	31.4±2.0	59.5±2.4				-
	31.5±1.0	68.2±3.8				
	34.1±1.6	73.5±4.2				
	Average	32.3±3.0	67±14			
Total carbon^{c,d} (%)		28				
33DMbutanone + OH + NO ^f	121.1±6.7	-	-		2.01	Acetone
	161.9±19.7	-	-		2.55	Nitrated compound
	89.2±6.4	-	-		9.04	2,2 dimethyl 3-propyl-oxynitrite
	Average^g	93.0±72.8	-	-	14.62	Nitrated compound
Total carbon^{c,d} (%)		47				

Con formato: Inglés (Estados Unidos)

Con formato: Inglés (Estados Unidos)

Con formato: Inglés (Estados Unidos)

Con formato: Inglés (Estados Unidos)

Con formato: Inglés (Estados Unidos)

Con formato: Inglés (Estados Unidos)

Con formato: Inglés (Estados Unidos)

Con formato: Inglés (Estados Unidos)

Con formato: Inglés (Estados Unidos)

Con formato: Inglés (Estados Unidos)

Con formato: Inglés (Estados Unidos)

Con formato: Inglés (Estados Unidos)

Con formato: Inglés (Estados Unidos)

^aYields have been estimated using the reference IR spectra from the Eurochamp database (Rodenäs et al., 2017). ^bThe rate coefficient used to correct the concentration of formaldehyde has been $k_{CF} = 7.2 \times 10^{-11} \text{ cm}^3 \text{ molecule}^{-1} \text{ s}^{-1}$ from IUPAC(2017). ^c $\text{Total carbon} = \frac{\sum_i \text{no. of carbon of product}_i}{\text{no. of carbon of 33dmbutanone}} \times \text{molar yield}_i$. ^dNitrated compounds have not been accounted for total carbons. ^eOnly FTIR experiments using H₂O₂ as OH radical precursor. ^fExperiments using methyl nitrite as OH radical precursor. ^gThe acetone yield must be taken with caution due to interference with IR bands of methyl nitrite.

The yield of HCHO and nitrated compounds for the reaction of 33DMbutanal with OH radical has not been determined, as there is a significant contribution from other sources such as the precursor used to generate the OH radical (which is a nitrated compound, methyl nitrite) and its degradation (which generates methyl nitrate and formaldehyde).

⁽⁺⁾ Little Peaks

^gGC-TOFMS experiments. The retention time shorter than Cl+NO and OH experiment due to the use of a different chromatographic column. The positive identification and quantification were not possible due to the scarce of commercial standards.

1 Table 4. Estimated yields (%) for reaction products formed in the reactions of 33DMbutanal with Cl atoms in the absence and in the presence of NO and with NO₂ and OH radical
 2 using FTIR and the product identify in the qualitative analysis using GC TOFMS.

Reaction	FTIR				GC TOFMS	
	Yield 2,2DMpropanal ^a (%)±2σ	Yield acetone (%)±2σ	Yield HCHO ^{b,c} (%)±2σ	Yield Nitrated comp. (%)±2σ	tr minutes	Reaction Product
33DMbutanal + Cl	28.4±0.4	31.1±0.6	37.4±0.3	-	2.2	Acetone
▲	29.6±0.3	26.8±0.4	38.5±0.4	-	2.65	Hydroxyacetone
▲	29.9±2.0	27.5±0.3	40.5±1.0	-	3.42	22DMpropanal
Average	29.3±0.7	28.5±2.4	38.8±1.5	-	5.82	22DMpropanol
Total carbon ^d (%)	45				8.23	22DMbutanodial/22DMpropanoic acid**
					9.57	33DMbutanoic acid
					13.25	2,2 DMtetrahydrofuranone
					15.78	4-hydroxi 3,3DMbutanal or (2,3 dihydro 4,4-DMfuran)
					16.14	3-hydroxy 2,2 DMpropanal
33DMbutanal + Cl + NO	12.8±2.6	20.3±0.6	83.3±1.9	52.1±3.1	2.2	Acetone
▲	7.7±0.2	20.8±0.3	89.2±1.4	50.3±3.2	3.41	22DMpropanal
▲	7.6±0.2	22.4±1.0	95.3±3.1	52.5±2.0	5.82	22DMpropanol
Average	9.4±3.0	21.1±1.1	89.3±6.0	51.6±1.2	6.97	peroxy 3,3 dimethylbutyryl nitrate
Total carbon ^{d,e} (%)	33.2				8.26	33DM-oxo-butanal/22DM-propanoic acid**
					9.58	33DMbutanoic acid
					13.25	2,2 DMtetrahydrofuranone
					16.16	3-hydroxy 2,2 DMpropanal
33DMbutanal + NO ₂	Not observed	Not observed	Not observed	100	2	Acetone
					3.08*(3.42)	2,2DMpropanal
					5.47*(5.82)	2,2DMpropanol
					6.68*(6.97)	peroxy 3,3 dimethylbutyryl nitrate
					7.15	Nitrated compound

Con formato: Inglés (Estados Unidos)

Con formato: Inglés (Estados Unidos)

Con formato: Inglés (Estados Unidos)

Con formato: Inglés (Estados Unidos)

Con formato: Inglés (Estados Unidos)

Con formato: Inglés (Estados Unidos)

Con formato: Inglés (Estados Unidos)

Con formato: Inglés (Estados Unidos)

Con formato: Inglés (Estados Unidos)

Con formato: Inglés (Estados Unidos)

Con formato: Inglés (Estados Unidos)

Con formato: Inglés (Estados Unidos)

Con formato: Inglés (Estados Unidos)

				7.88*(8.23) 8.94 (9.56)	33DM-oxo-butanal/22DMpropanoic acid** 3,3-dimethylbutanoic acid	
33DMbutanal + OH	Not observed ^(†)	24.9±08	-	-	2 Acetone	
		34.6±1.0	-	-	7.16 Nitrated compound	
		37.1±0.7	-	-	8.92*(9.56) 33DMbutanoic acid	
Average		32.2±6.4	-	-		
Total carbon ^d (%)		16.1				

Con formato: Inglés (Estados Unidos)

Con formato: Inglés (Estados Unidos)

Con formato: Inglés (Estados Unidos)

Con formato: Inglés (Estados Unidos)

Con formato: Inglés (Estados Unidos)

1 ^aThe rate coefficient used to correct the concentration of 22DMpropanal has been $k_C=1.42\times10^{-10}\text{-cm}^3\text{-molecule}^{-1}\text{-s}^{-1}$ from Calvert et al., 2011. ^bYields has been estimated using the reference IR
2 spectra from the Eurochamp database (Rodenas et al., 2017). ^cThe rate coefficient used to correct the concentration of formaldehyde has been $k_C=7.2\times10^{-11}\text{-cm}^3\text{-molecule}^{-1}\text{-s}^{-1}$ from IUPAC(2017). ^d
3 $Total\ carbon = \sum_i \frac{n^o\ of\ carbon\ of\ product_i}{\sum_i n^o\ of\ carbon\ of\ 33dmbutanal} \times molar\ yield_i$. ^eNitrated compounds have not been accounted for.
4 ^(††)Probable interference with IR bands of nitrated compounds.
5 The yield of HCHO and nitrated compounds has not been determined, as there is a significant contribution from sources other than the main reaction, such as the precursor used to generate the OH
6 radical (which is a nitrated compound, methyl nitrite) and its degradation (which generates methyl nitrate and formaldehyde).
7 [‡]GC-TOFMS experiments. Retention time shorter than CI experiments due to the use of a different chromatographic column. The positive identification and quantification was not possible to scarce
8 of commercial standards. Only 22DMpropanal was confirmed with standard.
9
10

As shown in Tables 3 and 4, the range of total carbon recovered is less than 100%. Only in the case of the reaction of 33DMbutanone with Cl atoms in the presence of NO the total carbon is 95% (not accounting for nitrated compounds), but it is important to note that the residual FTIR spectra (see Figure 8S) indicate the presence of other compounds that are not accounted for total carbon. The residual spectra magnified (see Figure 9S) shows IR absorption bands that can be assigned to reaction products proposed in the general Scheme 1S as formic acid and hydroxyacetone. On the other hand, it is interesting to note that in the residual spectra for the reaction of 33DMbutanal with the three oxidants, showed in Figure 10S, some IR absorption bands appear at the same wavenumber indicating common reaction products.

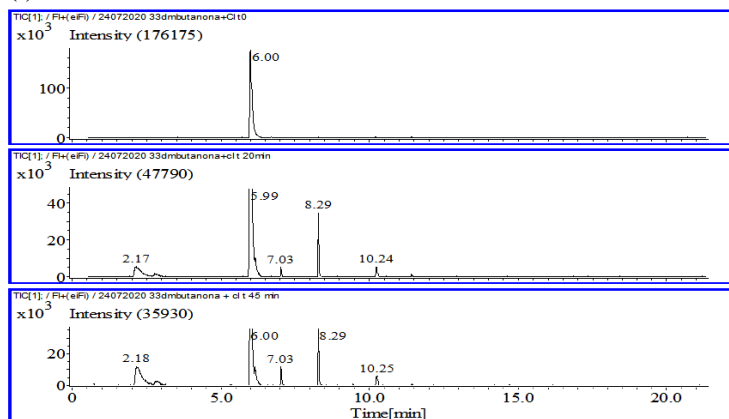
Gas chromatography coupled with a time-of-flight mass spectrometer (GC-MSTOF) using EI and/or FI ionization mode has been employed as a complementary technique to FTIR to identify more reaction products or to confirm those detected by FTIR. The yields should be considered with caution due to potential systematic errors during the quantification analysis.

3.2.2 SPME/GC-TOFMS experiments

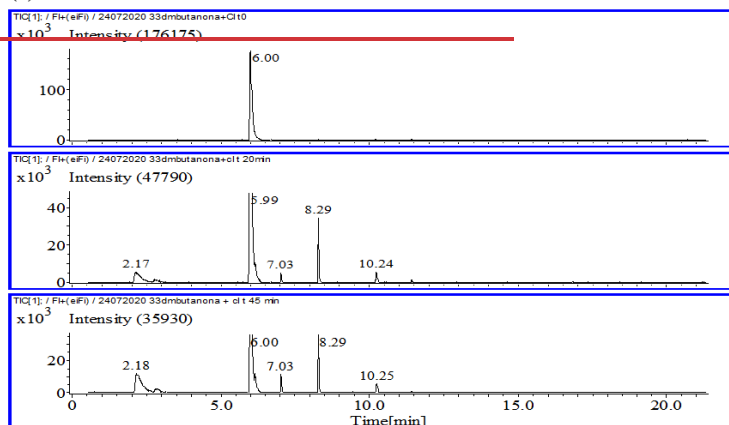
The SPME/GC-TOFMS chromatograms in Electron ionization mode (EI) collected at different reaction times for the studied reaction, show peaks at different retention times whose areas increase with the reaction time, indicating that they correspond to reaction products. (Figure 11S). Due to the characteristic of SPME sampling method, only a qualitative analysis was possible.

For the reaction of 33DMbutanone with Cl atoms in the presence and the absence of NO, also GC-MS analysis using Field Ionization was carried out. The FI mass spectrum helps to establish the identification of reaction products. Figure 6 shows an example of the SPME/GC-TOFMS chromatograms collected in FI and EI mode for the reaction of 33DMbutanone with Cl.

(a)



(b)



(c)

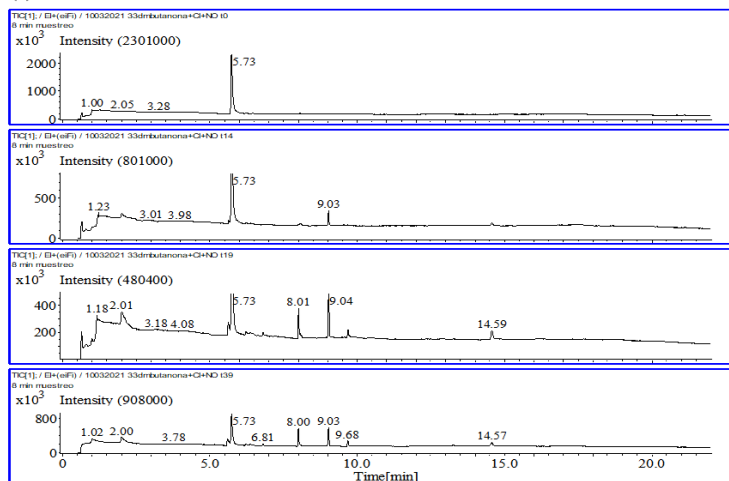


Figure 6. Example of the SPME/GC-TOFMS chromatograms for the reaction of 33DMbutanone + Cl atoms (a) in the absence of NO and FI mode, (b) in the presence of NO and FI mode and (c) in presence of NO and EI mode.

It can be observed that the FI chromatograms in the absence of NO (a) present more peaks than the corresponding ones in the presence of NO (b), with only one peak being common ($t_r = 8.29$ min). This indicates that the presence of NO influences the reaction mechanism. In the case of the chromatograms obtained under the same reaction conditions but with different ionization modes ((b) and (c) chromatograms), a different number of peaks also is observed, probably because some reaction products were not ionized with FI (peaks at $t_r = 9.68$ and 14.57). Additionally, the peak in chromatogram (a) and (b) of 33DMbutanone appears at shorter retention times than in chromatogram (c), due to the use of a different chromatographic column. Taking into account this, the peaks at $t_r = 2.24$; 6 ; and 8.29 min, showed in chromatograms (b) correspond with the peaks at $t_r = 2$; 5.73 ; 8.0 and 9.03 min in chromatograms (c).

The mass spectrum of each peak was analysed using the NIST database of GC-MS or comparing with the mass spectrum of the commercial sample. In some cases, the positive identification with high percentage of similitude index were obtained but in other cases, only a tentative assignation was possible based on profile of fragments m/z generated and the reaction products expected according to the schemes 1S and 2S proposed. In those cases, in which FI spectrum could be obtained, the assignation was made based on fragment m/z of molecular weight. All chromatograms collected in EI mode present a little peak that appear together with the peak of air, that could correspond to acetone. In order to confirm the presence of acetone to this retention time (~ 2 min) a chromatogram has been created using a specific tool of the software of mass spectrometer. For that, in the software it is specified the desired m/z (58 m/z for acetone) and then the chromatogram is generated, displaying the ion intensity versus time, with peaks representing the compounds that correspond to the specified m/z . With this tool the experimental chromatograms have been modified in for a better analysis of all chromatographic peaks. Prior to the mass spectra analysis, it was verified that the experimental and generated chromatograms were identical. In the supplementary material, the GC-TOFMS chromatograms generated with this tool for all reactions are compiled (Figures 12S-16S).

The mass spectra of all chromatographic peaks are presented in Tables 2S-3S for the reactions of 33DMbutanone and 33DMbutanal, respectively. An assignment of the reaction products corresponding to each peak has been made, taking into account schemes 1S, 2S and the results of FTIR experiments. However, due to the unavailability of commercial samples, the formation of some product proposed could not positively confirmed. Only in the reaction of 33DMbutanal, the injection of a real sample of 22DMpropanal, allowed the confirmation of this product assigned to a peak at $t_r = 3.08/3.41$ minutes.

The SPME/GC-TOFMS experiments show the formation of the main compounds quantified in the FTIR experiments, such as acetone and 2,2-dimethylpropanal (22DMpropanal) in the case of the 33DMbutanal reactions. Due to the SPME sampling procedure, formaldehyde could not be detected. The formation of other organic compounds, generally multifunctional of varying alkyl chain lengths, (hydroxycarbonyls, oxocarbonyls, hydroxy-oxo-carbonyls, organic acids) is observed. These compounds could correspond to the unidentified compounds in the FTIR spectra.

Next a discussion of the results on reaction products with both analytical techniques for each of the compounds studied is presented.

3.2.2.1 33DMbutanone reaction products

In the SPME/GC-TOFMS chromatograms for the reactions of 33DMbutanone (Figures 6, 12S) can see that the number of peaks and therefore the reaction products generated is different. Based on the retention times and mass spectra summarized in Table 2S, similar compounds seem to be formed in these reactions.

As shown in Table 3, the percentage of acetone and formaldehyde in the reactions with Cl and OH in the presence of NO is higher than in experiments without NO. This indicates that, in the presence of NO, the formation of the alkoxy radical by reaction of the peroxy radical (RO_2) with NO is favored, compared to the formation of this same alkoxy radical by self-reaction of RO_2 . Additionally, these alkoxy radicals are chemically activated and undergo 'prompt' decomposition to form acetone, in contrast to alkoxy radicals formed by the self-reaction of RO_2 , which are more thermally stabilized (Atkinson et al., 2007). In the reactions of 33DMbutanone in the absence of NO, the percentage of acetone is lower in the OH reaction than Cl reaction, which could be explained by the possible reaction of RO_2 with OH radical present in the reaction medium, to form RO_2OH rather than RO_2 reacting with itself to yield two alkoxy radicals. The IR band observed at $\sim 1800\text{ cm}^{-1}$ for 33DMbutanone + Cl reaction could correspond with the stretching vibration of the C=O (carbonyl) bond in acyl chloride. This compound can be formed by the reaction of RO_2 with Cl_2 or Cl atoms (Ren et al., 2018). In the Cl reaction without NO, the identification of a product with a molecular mass of $m/z=116$ (at $t_r=10.26\text{ min}$), assigned to 4-hydroxy-3,3-dimethyl-2-butanone (see Table 2S), is explained by the self-reaction of two RO_2 radicals, leading to the formation of two molecules. In this case, the co-product molecule to 4-hydroxy-3,3-dimethyl-2-butanone would correspond to a compound with a molecular weight of $m/z=114$ (at $t_r=8.28$), assigned to 2,2-dimethyl-2-oxo-butanal. This compound is also observed in the Cl reaction in the presence of NO, formed by the reaction of the alkoxy radical with O_2 . The peak at $t_r=2.55\text{ min}$ with a mass of $m/z=72.08$ (Table 2S), assigned to hydroxyacetone, the peak at $t_r=7.03\text{ min}$ with a molecular mass of $m/z=102$, assigned to 1-hydroxybutan-2,3-dione, and the IR absorption band at 1105.42 cm^{-1} (see Figure 10S), characteristic of formic acid, indicate that the alkoxy radical also undergoes different isomerization processes.

The reaction of 33DMbutanone with Cl and OH in the presence of NO (at short times) and NO_2 (at long times) leads to the formation of chromatographic peaks at $t_r=5.59, 9.04, 9.68$, and 14.62 min for the Cl reaction, and $t_r=2.55, 9.04$, and 14.62 min for the OH reaction, which have been assigned to nitrated compounds (also observed in the FTIR experiments). Specifically, the peak at 5.59 minutes has been assigned to peroxyacetyl nitrate (PAN). Additionally, based on the IR bands observed in the residual spectra at times less than 5 minutes for the Cl and OH reaction in the presence of NO, other nitrated compounds are assigned as alkoxy-nitrates (IR band around 850 cm^{-1}). The formation of PAN can only be explained through the channel II, with the decomposition of the initially formed alkoxy radical (2,2-dimethyl-3-oxobutan-1-yloxy radical). The estimated yield for PAN of 100% indicates that the percentage of Cl attack on the $-CH_3$ of the tert-butyl group is 100%, a value very close to the 98% estimated by the SAR method for reactions with Cl (see Table 1S).

For the reactions with OH, only acetone and formaldehyde have been quantified. These products may come from OH attack on the methyl of the tertiary carbon of 3,3-dimethylbutanone (channel II) or on the methyl directly attached to the carbonyl group (channel I). Thus, this study cannot confirm that 94% of the reaction proceeds through channel II, as the SAR method suggests. However, considering that the rate coefficient estimated by the SAR method is similar to that obtained in this study, channel II can be considered the main process. From the analysis of the SPME/GC-TOFMS experiments, the proposed reaction products also are listed in Table 3. Based on the kinetic results and the main products obtained in this study, the reaction mechanism showed in Figure 7 is proposed for the degradation of 3,3-dimethylbutanone.

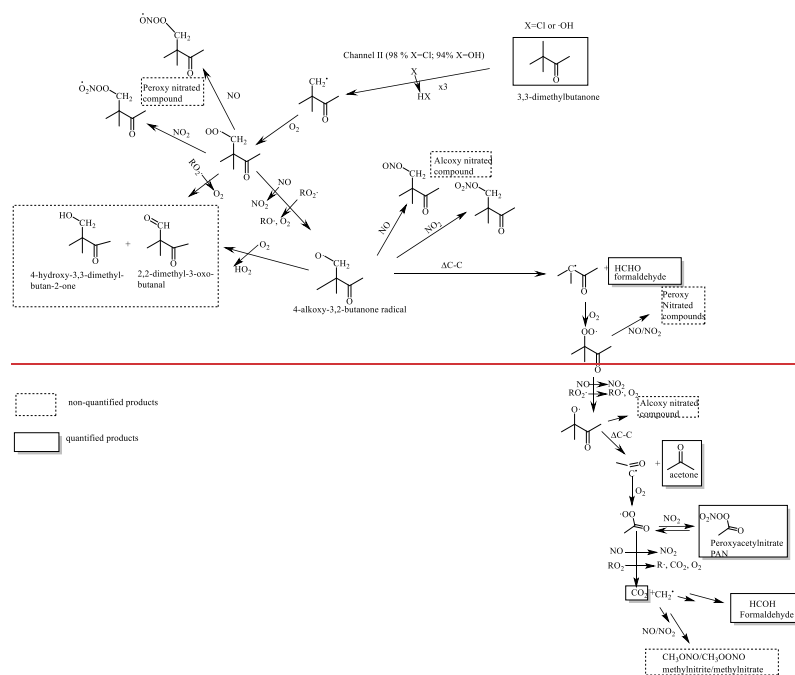


Figure 7. Mechanism proposed by the formation of the main reaction products observed for 3,3-dimethylbutanone reactions with Cl atoms and OH radical. The framed products correspond to products identified by FTIR and/or SPME/GC-TOFMS.

3.2.2.2 33DMbutanal reaction products

In the analysis of SPME/GC-TOFMS chromatograms, the number of peaks observed with appreciable intensity in the reaction of Cl atoms in the presence of NO (10 peaks), in the absence of NO (8 peaks), and in the NO₃ reaction (7 peaks) is greater than in the reaction with OH, where only 3 peaks are observed (see Figures 13S-16S). This fact may be related to the different attack positions of the oxidant when reacting with 33DMbutanal: 3 for the reaction with Cl atoms, 2 for the reaction with the NO₃ radicals, and 1 for the reaction with the OH radicals, as estimated by the SAR method (see Table 1S). Some of these peaks appear at the same retention times, and their mass spectra are very similar (see Table 2S), indicating that they are the same reaction products. Some of these products are also identified in the FTIR analysis (see Table 4); such as acetone (*t_r* = 2.2 min) and 22DMpropanal (*t_r* = 3.08 or 3.43 min).

It is interesting to note the presence of a common peak for all reactions that appears at 9.56 min (8.95 min in the experiment with a new chromatographic column). The mass spectrum of this peak is assigned to 3,3-dimethylbutanoic acid by the NIST database software, with a similarity index of approximately 84%. This compound cannot be explained by the general scheme proposed (Scheme 2S), which is based on principles of atmospheric reactivity and bibliographic studies of similar compounds (Aschmann et al. 2010, Atkinson et al. 2007). In order to explain the formation of this peak, other pathway was proposed, where the oxy-3,3-dimethylbutyryl radical (channel I), undergoes isomerization. This pathway leads to the formation of 4-oxo-3,3-dimethylbutanoic acid, whose mass spectrum shows a fragmentation pattern very similar to the peak with a *t_r* of 9.56 min. In order to establish which compound corresponds to this peak and taking into account that 3,3-dimethylbutanoic acid (33DMbutanoic acid) is a commercial compound, a sample of 33DMbutanoic acid was injected into the SPME/GC-TOFMS system. The analysis showed a chromatogram with a peak at approximately 9 minutes, with a mass spectrum (MS) identical to that of the peaks (9.56/8.95 min), which positively confirms the formation of this 3,3-dimethylbutanoic acid in the reactions of 33DMbutanal with atomic Cl and OH and NO₃ radicals (See Figure 17S). The characteristic IR bands of 33DMbutanoic acid seem to be present in the FTIR residual spectra obtained for the reaction of 33DMbutanal with Cl atoms (Figure 18S). Recent studies have also detected organic acids from reactions of saturated aldehydes (Asensio et al. 2022, Bo et al. 2022).

The remaining chromatographic peaks showed in Figures 13S-16S, have been assigned to reaction products shown in the general Scheme 2S. Table 3S contains all the mass spectra and their assignments. In general, the complete interpretation of mass spectra is complex because the formed products have very similar structures, leading to similar fragmentation patterns. The mass spectrum of chromatographic peaks around 8 min (7.88, 8.23, and 8.26 min) could correspond to several structurally similar products. The injection of a commercial sample of 2,2-dimethylpropanoic acid (22DMpropanoic acid) in the SPME/GC-TOFMS system shows a peak with a retention time of 8 min, whose mass spectrum correspond with the mass spectrum of the peak at 8.23 min observed in the reaction of 33DMbutanal with Cl atoms in the absence of NO. Figure 16S, shows an IR reference spectrum of 22DMpropanoic.

As can be seen in Table 3S, some of the proposed reaction products are dicarbonyls or hydroxycarbonyl compounds. The hydroxycarbonyl compounds tend to cyclize to dihydrofurans via acid-catalyzed heterogeneous reactions (Atkinson et al. 2008). For example, 4-hydroxy-3,3DMbutanal (*t_r* = 15.78 min)

can cyclize to form 2,3 dihydro 4,4 dimethylfuran. Another cyclization process can occur from an alkoxy carbonyl radical, such as the 4 formyl 2,2 dimethylbutan-1-yloxy radical, leading to the formation of 2,2 dimethyltetrahydrofuran 2-one ($t_r = 13.25$ min).

The common chromatographic peak at 6.97/6.86 min observed in the Cl + NO and NO₃ reactions has been assigned to a nitrated compound, which could correspond to peroxy-3,3 dimethylbutyryl nitrate also detected in the FTIR analysis. The intensity of these peaks is very low, likely because the compound undergoes thermal decomposition in the chromatograph injector. Another small chromatographic peak at 7.15 min observed in the NO₃ and OH radical reactions could correspond to two nitrated compounds with the same retention time: peroxy nitrite (in the case of the OH reaction) and peroxy nitrate (for the NO₃ reaction), according to the characteristic IR bands of peroxy compounds at 793 cm⁻¹ observed in the FTIR spectra (see Figure 10S). Figure 10S also shows an IR band at 810 cm⁻¹ for the Cl + NO and OH reactions, which is characteristic of alkoxy nitrated compounds. This common product was not detected in SPME/GC-TOFMS, possibly because it was not adsorbed onto the fiber. In general, SPME/GC-TOFMS is not an effective sampling method for nitrated compounds.

Table 4 provides a summary of the reaction products tentatively assigned to the chromatographic peaks observed in the experiments conducted for the reactions of 33DMbutanal with atmospheric oxidants, along with the products identified and quantified using FTIR.

Finally, the analysis of the quantified compounds in the FTIR experiment can provide insights into the percentage of each channel or which pathway is favored. Acetone is a reaction product that, according to Scheme 2S, is formed from all channels. However, the similar yields in the Cl, Cl + NO, and OH reactions (28%, 21%, and 32%, respectively) may indicate that acetone is formed from all reactions primarily through channel I. HCHO is also a product formed through all three channels, but the highest yield of formaldehyde, along with the significant decrease of 22DMpropanal obtained in the reaction of Cl in the presence of NO compared to the yields of these compounds for the reaction of chlorine in the absence of NO, could indicate that, in the presence of NO, the reaction of the peroxy species generated in channel I or channel II to form nitrated compounds is favored at the expense of the self-reaction of RO₂.

The total carbon calculated for the Cl reaction in the absence of NO, based on the yields of HCHO, acetone, and 22DMpropanal, accounts for only 45%. The remaining carbon can be explained by the formation of other compounds identified through SPME/GC-TOFMS. Additionally, the IR band at 1105 cm⁻¹ shown in Figure 11S in the FTIR spectrum of the Cl atoms reaction in the absence of NO, indicates the formation of formic acid, which was not quantified. The lower yields in the Cl reaction in the presence of NO (33%) and OH (16%) could be attributed to the significant formation of nitrated compounds, whose yield has not been included in the total carbon calculation. For the NO₃ radical reaction, the linear trend observed in Figure 5 indicates that nitrated compounds are formed through the main reaction, and therefore, 100% of the reacted 33DMbutanal forms nitrated compounds in this reaction conditions. The identification of other compounds in the SPME/GC-TOFMS analysis could be due to the rapid decomposition of peroxy nitrated compounds in the chromatograph's injection port or an overestimation of nitrated compound yields. To determine if these products are generated in significant amounts, quantification is necessary, but this is not possible due to the lack of standards or the characteristics of the SPME sampling method.

No exclusive compounds to each reaction channel (I, II, or III) have been quantified for 3,3DMbutanal reaction. Therefore, it is not possible to determine the percentage of each channel through which the reaction of 3,3DMbutanal with each oxidant proceeds. The formation of 3,3DMbutanoic acid in all reactions implies other reaction pathway that has not been considered. The following reaction has been proposed as possible pathways to explain the formation of the 3,3-dimethylbutanoic acid ((CH₃)₃CCH₂C(O)OH):



Similar reaction was proposed for CH₃C(O)OO radical by some authors (Dillon and Crowley 2008, Groß et al., 2014, Tomas et al., 2001). On the other hand, 2,2DMpropanoic acid (observed in the 3,3DMbutanal with Cl atoms) could be a secondary product formed from the degradation of 2,2DMpropanal. The yields of organic acids from the corresponding aldehyde must be very low (Bo et al. 2022), and therefore, the pathway (R2) must be a minority channel.

From the analysis of the SPME/GC-TOFMS experiments, the proposed reaction products are also listed in Table 3. Based on the products identified in this work, the previous bibliographic study of 3,3DMbutanal with the OH radical (Aschmann et al. 2010) and considering the estimated percentages for each channel using the SAR method, the reaction mechanism for 3,3DMbutanal with Cl atoms, OH and NO₃ radicals showed in Figure 9, is proposed to explain the main observed reaction products in each reaction.

$$\tau_{ox} = \frac{1}{k_{ox}[Ox]} \quad (III)$$

where τ_{ox} represents the lifetime for the considered reaction, k_{ox} is the rate coefficient, and $[Ox]$ refers to the typical atmospheric concentration of the oxidant. The atmospheric lifetimes of 33DMbutanone and 33DMbutanal were calculated using the rate coefficients and the concentration of oxidant from ~~of~~ Table 2. For 33DMbutanal the k_{OH} and k_{NO_3} have been the averaged from the two rate coefficients available in the literature.

The ketones and aldehydes can significantly absorb light in the tropospheric actinic region $\lambda > 290$ nm, and the photolysis could play an important degradation process (Mellouki et al., 2015; Atkinson, 2003; Mellouki et al., 2015). There are not any experimental data about UV-Vis absorption cross-sections of 33DMbutanal that could allow the calculation of the photolysis rate. The value of $J(0, \theta) = 3 \times 10^{-5} \text{ s}^{-1}$ calculated for 3-methyl-butanal (similar compound to 33DMbutanal) by Lanza et al. (2008), has been used to estimate the photolysis lifetime. For 33DMbutanone a photolysis rate of $J(z, \theta) = 2.4 \times 10^{-6} \text{ s}^{-1}$ was estimated by Mapelli et al., (2023).

Regarding the deposition process, the lifetime associated with wet deposition could be estimated with the Eq. (IV) by (Chen et al., 2003):

$$\tau_{wet} = \frac{H_{atm}}{k_H v_{pm} RT} \quad (IV)$$

where k_H is the Henry's law constant; H_{atm} is the height in the troposphere ($H_{atm} = 630$ m), v_{pm} is the average precipitation rate (536 mm yr^{-1} for Spain, (<http://www.aemet.es>, last access: 4 October 2024), R is the gas constant ($8.14 \text{ Pa m}^3/\text{mol K}$); and T is the temperature, considered to be constant and equal to 298 K . In the literature, there is only one data of Henry's constant for 33DMbutanone of $4.3 \times 10^{-2} \text{ mol/m}^3\text{Pa}$ (Sander, 2023, Hovorka et al., 2019, Sander, 2023) which has been used for 33DMbutanal as well. ~~The same data has been used to 33DMbutanal.~~

Taking into account all those degradation processes, a global lifetime (τ_{global}) has also been calculated for 33DMbutanone and 33DMbutanal with the the Eq. (IV):

$$\tau_{global} = \left[\frac{1}{\tau_{Cl}} + \frac{1}{\tau_{OH}} + \frac{1}{\tau_{NO_3}} + \frac{1}{\tau_{phot}} + \frac{1}{\tau_{wet}} \right]^{-1} \quad (IV)$$

Table 5. Atmospheric lifetimes of 33DMbutanone and 33DMbutanal.

	^a τ_{Cl} (days)	τ_{Cl}^* (days)	^b τ_{OH} (days)	^c τ_{NO_3} (days)	τ_{phot} (days)	τ_{wet} (years)	τ_{global} (days)	[*] τ_{global} (days)
33DMbutanal	91	0.7	0.5	1.2	0.4 ^d	11	0.2	0.14
33DMbutanone	274	2.1	9.2	-	5 ^e	11	2.5	1.14

^aDetermined using the 24 h average $[Cl] = 1 \times 10^3 \text{ atoms cm}^{-3}$ (global average) (Platt and Jansen, 1995). ^{*}Determined using the peak of $[Cl]$ in coastal and industrial areas at $1.3 \times 10^5 \text{ atoms cm}^{-3}$ (Spicer et al., 1998). ^b Determined using the 12 h average of $[OH \cdot] = 1 \times 10^6 \text{ radicals cm}^{-3}$ (12-hour average) (Prinn et al., 2001), $[NO_3 \cdot] = 5 \times 10^8 \text{ radicals cm}^{-3}$ (Atkinson, 2000). ^dData calculated with a J from Lanza et al., 2008. ^eData calculated with a J from Mapelli et al., 2023.

Con formato: Color de fuente: Rojo

Con formato: Fuente: Cursiva, Color de fuente: Rojo

Con formato: Fuente: Cursiva, Color de fuente: Rojo

Con formato: Fuente: Cursiva, Color de fuente: Rojo

Con formato: Color de fuente: Rojo

Con formato: Color de fuente: Rojo

Con formato: Color de fuente: Rojo

It can be observed that the dominant tropospheric loss processes of 33DMbutanone and 33DMbutanal are their reactions with OH radicals and photolysis process (note that photolysis lifetime depends on the atmospheric conditions considered), followed by their reaction with NO₃ radicals at night. However, in places where there is a peak concentration of Cl atoms (coastal areas), the reaction with Cl atoms may compete with photolysis and reaction with OH radicals as their main degradation process. The calculated wet lifetime of 11 years indicate that the wet deposition can be considered negligible.

The shorter global lifetimes of ~4 hours for 33DMbutanal and ~ 2 days for 33DMbutanone indicate that these compounds are degraded near their generation sources. The products created in the degradation reactions of 33DMbutanone and 33DMbutanal may also have environmental implications. Thus, formaldehyde is classified as potentially carcinogenic to humans (NTP, 2021). Acetone, 22DMpropanal and organic nitrates (PAN and peroxybutyrylnitrate) are also key components in photochemical smog episodes, a major contemporary environmental issue. The multifunctional compounds such as oxocarboxyls, dicarbonyls, hydroxycarbonyls and organic acids are products with polar groups characterized by low volatility, which could facilitate the formation of secondary organic aerosols (SOA) (Asensio et al., 2022, Calvert et al., 2011, Asensio et al., 2022). Moreover, the nitrated compounds generated can act as NO_x reservoir species, especially during the night (Altshuller, 1993) and could have an influence on global scale.

The potential for ozone formation of 33DMbutanone and 33DMbutanal has been evaluated calculating their Photochemical Ozone Creation Potential (POCP) according to the method of Jenkin et al. (2017). The Photochemical Ozone Creation Potential estimated (POCP_E), were 68 and 58 for conditions in NW Europe and urban areas of the USA, respectively for 33DMbutanal and 26 and 15 for conditions in NW Europe and urban areas of the USA, respectively for 33DMbutanone. Comparing with other series of organic compounds (Jenkin et al., 2017), the values of POCP_E for 33DMbutanal indicate that it is an important contributor to tropospheric ozone generation.

Regarding the calculation of the GWP (global warming potential) parameter, the method of Hodnebrog et al. (2020) and the lifetime calculated above have been used to estimate the GWP of 33DMbutanone. A value of 0.13 for a time horizon of 20 years has been obtained, and therefore, the direct contribution to the radiative forcing of climate can be considered negligible. The GWP for 33DMbutanal has not been calculated because its lifetime is shorter than that of 33DMbutanone, and thus, its expected GWP is likely to be lower.

5 Conclusions

In this work, the rate coefficient for the reaction of 33DMbutanal with Cl atoms has been determined for the first time. Additionally, the rate coefficients for 33DMbutanone with Cl atoms and the OH radicals have been measured, aligning with existing literature data. The kinetic findings, along with previous studies on other carbonyl compounds, confirm that reactivity is influenced by the type of carbonyl group (aldehyde vs. ketone) and the number and position of methyl groups. This research has expanded the database on these compounds, especially regarding their reactions with Cl atoms.

The study of reaction products using FTIR and GC-TOFMS allows to identify and quantify acetone, formaldehyde, and 2,2-dimethylpropanal, alongside multifunctional products like hydroxycarbonyl, oxocarbonyl, and nitrated compounds such as PAN and peroxybutyryl nitrate. The differing acetone yields from 3,3-dimethylbutanone with Cl atoms and OH radical suggest the importance of the $\text{RO}_2 + \cdot\text{OH}$ reaction in unpolluted atmospheres. The results suggest that the $\text{RO}_2 + \text{OH}$ reaction in the unpolluted atmosphere could be significant. The proposed mechanism for 3,3-dimethylbutanone indicates that hydrogen abstraction from the tert-butyl methyl group is the primary pathway for Cl and OH, confirming SAR predictions. In the 3,3-dimethylbutanal reaction, hydrogen abstraction occurs from various functional groups depending on the reacting species (Cl atoms, OH and NO_3 radicals), also aligning with SAR predictions. The positive identification of 3,3-dimethylbutanoic acid implies a pathway in the reaction mechanisms of 3,3-dimethylbutanal, that initially have not been considered.

The atmospheric conditions determine the reaction products obtained in the atmospheric degradation of 3,3-dimethylbutanal and 3,3-dimethylbutanone. Thus, in polluted environments with high concentrations of NO_x , nitrated organic compounds (RONO_2) are formed. Moreover, when the concentration of NO_2 is higher than that of NO, ozone is formed. In a clean atmosphere, as in the case of the experiments with Cl atoms in the absence of NO_x , the reaction products are hydroxy/oxo carbonyl compounds.

Atmospherically, both 3,3-dimethylbutanal and 3,3-dimethylbutanone degrade within a few hours and 2 days respectively during the day, implying that degradation happens close to the emission sources. Their direct contribution to radiative forcing is minimal. However, their estimated POCP values suggest a potential role in tropospheric ozone formation, especially for 3,3-dimethylbutanal. The multifunctional products formed may contribute to secondary organic aerosol formation, and their further oxidation in the troposphere could enhance photochemical smog, impacting air quality and human health.

Data availability. The underlying research data are available upon email request from the contact author of this work.

Supplement. The electronic Supplement includes additional tables and figures.

Author contributions.

Inmaculada Aranda: Formal analysis, validation, investigation, methodology, writing-original draft.

Pilar Martín: Conceptualization, supervision, methodology, writing-original draft. **Sagrario Salgado** Conceptualization, supervision, methodology, writing-original draft. **Florentina Villanueva:** Supervision, methodology. **Beatriz Cabañas:** Conceptualization, supervision, funding acquisition.

Acknowledgments

The authors thank for financial support. I. Aranda thanks UCLM for funding her research contract (Plan Propio de I+D+i) cofinanced by FSE. The authors would like to thank Dr. Diana Rodriguez for her help in carrying out some of the experiments.

Financial support. This research has been supported by the Ministry of Science, Innovation and Universities (Project RTI 2018-099503-B-I00) and the Junta de Comunidades de Castilla-La Mancha (Project SBPLY/21/180501 /000283).

References

-Altshuller, A. P.: PANs in the Atmosphere, *Air & Waste*, 43, 1221–1230, <https://doi.org/10.1080/1073161X.1993.10467199>, 1993.

~~-Aranda, I., Salgado, S., Martín, P., Villanueva, F., Pinés, M.T., Cabañas, B.: Atmospheric degradation of 2-Isopropoxyethanol: Reactions with Cl, OH and NO₃, *Atmos. Environ.*, 324–329, <https://doi.org/10.1016/j.atmosenv.2024.120420>, 2024.~~

-Aranda, I., Salgado, S., Martín, P., Villanueva, F., Martinez, E., Cabañas, B: Atmospheric degradation of 3-ethoxy-1-propanol by reactions with Cl, OH and NO₃, *Chemosphere*, 281, 130755–130764, <https://doi.org/10.1016/j.chemosphere.2021.130755>, 2021.

-Aschmann, S. M., Arey J., Atkinson, R: Kinetics and Products of the Reactions of OH Radicals with 4,4-Dimethyl-1-pentene and 3,3-Dimethylbutanal at 296 ± 2 K, *J. Phys. Chem. A*, 114, 18, 5810–5816, <https://doi.org/10.1021/jp101893g>, 2010.

-Asensio, M., Antiñolo, M., Blázquez, S., Albaladejo, J., and Jiménez, E.: Evaluation of the daytime tropospheric loss of 2-methylbutanal, *Atmos. Chem. Phys.*, 22, 2689–2701, <https://doi.org/10.5194/acp-22-2689-2022>, 2022.

-Atkinson, R.: Rate constants for the atmospheric reactions of alkoxy radicals: An updated estimation method, *Atmos. Environ.*, 41, Issue 38, 8468–8485, <https://doi.org/10.1016/j.atmosenv.2007.07.002>, 2007.

-Atkinson, R.: Atmospheric Degradation of Volatile Organic Compounds. *Chem. Rev.* 103, 12, 4605–4638, <https://doi.org/10.1021/cr0206420>, 2003.

-Atkinson, R.: Atmospheric chemistry of VOCs and NO(x). *Atmos. Environ.* 34, 2063–2101, [https://doi.org/10.1016/S1352-2310\(99\)00460-4](https://doi.org/10.1016/S1352-2310(99)00460-4), 2000.

-Atkinson, R., Arey J., Aschmann S. M: Atmospheric chemistry of alkanes: Review and recent developments, *Atmos. Environ.* 42(23), 5859–5871, <https://doi.org/10.1016/j.atmosenv.2007.08.040>, 2008.

-Bao, J., Li, H., Wu, Z., Zhang, X., Zhang, H., Li, Y., Qian, J., Chen, J., Deng, L: Atmospheric carbonyls in a heavy ozone pollution episode at a metropolis in Southwest China: Characteristics, health risk assessment, sources analysis, *J. Environ. Sci (China)*, 113, 40–54, <https://doi.org/10.1016/j.jes.2021.05.029>, 2022.

-Berndt, T., Scholz, W., Mentler, B., Fischer, L., Herrmann, H., Kulmala, M., Hansel, A.: Accretion Product Formation from Self- and Cross-Reactions of RO₂ Radicals in the Atmosphere, *Angew. Chem. Int. Ed.* 26;57(14):3820–3824. <https://doi.org/10.1002/anie.201710989>, 2018.

Código de campo cambiado

-Bo, S., Weigang, W., Cici, F., Yuchan, Z., Zheng, S., Yanli, Z., Maofa, G.: Study on the reaction of 3-methyl-2-butenal and 3-methylbutanal with Cl atoms: kinetics and reaction mechanism, *J. Environ. Sci.*, 116, 2022, 25-33, <https://doi.org/10.1016/j.jes.2021.03.032>, 2022.

-Bottorff, B., Lew, M. M., Woo, Y., Rickly, P., Rollings, M. D., Deming, B., Anderson, D. C., Wood, E., Alwe, H. D., Millet, D. B., Weinheimer, A., Tyndall, G., Ortega, J., Dusanter, S., Leonardis, T., Flynn, J., Erickson, M., Alvarez, S., Rivera-Rios, J. C., Shutter, J. D., Keutsch, F., Helmig, D., Wang, W., Allen, H. M., Slade, J. H., Shepson, P. B., Bertman, S., and Stevens, P. S.: OH, HO₂, and RO₂ radical chemistry in a rural forest environment: measurements, model comparisons, and evidence of a missing radical sink, *Atmos. Chem. Phys.*, 23, 10287–10311, <https://doi.org/10.5194/acp-23-10287-2023>, 2023.

-Byrne, F. P., Forier, B., Bossaert, G., Hoebbers, C., Farmer, T. J., and Hunt, A. J.: A methodical selection process for the development of ketones and esters as bio-based replacements for traditional hydrocarbon solvents, *Green Chem.*, 20, 4003–4011, <https://doi.org/10.1039/C8GC01132J>, 2018.

-Calvert, J. G., Mellouki, A., Orlando, J. J., Pilling, M. J., Wallington, T. J.: *The Mechanisms of Atmospheric Oxidation of the Oxygenates*. Oxford University Press, New York, 2011.

-Carter, W. P. L.: Estimation of Rate Constants for Reactions of Organic Compounds under Atmospheric Conditions, *Atmosphere*, 12, 1250. <https://doi.org/10.3390/atmos12101250>, 2021.

-Chen, L., Takenaka, N., Bandow, H., Maeda, Y.: Henry's law constants for C₂–C₃ fluorinated alcohols and their wet deposition in the atmosphere, *Atmos. Environ.*, 37, 34, 4817–4822, <https://doi.org/10.1016/j.atmosenv.2003.08.002>, 2003.

-Colmenar, I., Martín, P., Cabanas, B., Salgado, S., Tapia, A., Aranda, I.: Atmospheric fate of a series of saturated alcohols: kinetic and mechanistic study, *Atmos. Chem. Phys.* 20, 699–720. <https://doi.org/10.5194/acp-20-699-2020>, 2020a.

-Colmenar, I., Salgado, S., Martín, P., Aranda, I., Tapia, A., Cabanas, B.: 2020b. Tropospheric reactivity of 2-ethoxyethanol with OH and NO₃ radicals and Cl atoms. Kinetic and mechanistic study. *Atmos. Environ.* 224, 117367. <https://doi.org/10.1016/j.atmosenv.2020.117367>, 2020b.

-Colmenar, I., Martín, P., Cabanas, B., Salgado, S., Martínez, E.: Analysis of reaction products formed in the gas phase reaction of E,E-2,4-hexadienal with atmospheric oxidants: reaction mechanisms and atmospheric implications, *Atmos. Environ.* 176, 188–200. <https://doi.org/10.1016/j.atmosenv.2017.12.027>, 2018.

-D'Anna, B., Andresen, W., Gefen, Z., and Nielsen, C. J.: Kinetic study of OH and NO₃ radical reactions with 14 aliphatic aldehydes, *Phys. Chem. Chem. Phys.*, 3, 3057–3063, doi.org/10.1039/B103623H, 2001.

-D'Anna, B. and Nielsen, C. J.: Kinetic study of the vapour-phase reaction between aliphatic aldehydes and the nitrate radical, *J. Chem. Soc., Faraday Trans.*, 93(19), 3479–3483, <https://doi.org/10.1039/A702719B>, 1997.

-Dillon, T. J. and Crowley, J. N.: Direct detection of OH formation in the reactions of HO₂ with CH₃C(O)O₂ and other substituted peroxy radicals, *Atmos. Chem. Phys.*, 8, 4877–4889, <https://doi.org/10.5194/acp-8-4877-2008>, 2008.

-EUROCHAMP, 2020 <https://data.eurochamp.org/data-access/ir-spectra/#/>

-Farrugia, L. N., Bejan, I., Smith, S. C., Medeiros, D. J., and Seakins, P. W.: Revised structure activity parameters derived from new rate coefficient determinations for the reactions of chlorine atoms with a series of seven ketones at 290 K and 1 atm, *Chem. Phys. Lett.*, 640 87–93, <https://doi.org/10.1016/j.cplett.2015.09.055>, 2015.

-Finlayson-Pitts, B. J., Pitts, Jr. J. N.: *Chemistry of the Upper and Lower Atmosphere: Theory, Experiments, and Applications*. Academic Press, 2000.

-Fittschen, C.: The reaction of peroxy radicals with OH radicals, *Chem. Phys. Lett.*, 725, 102–108, <https://doi.org/10.1016/j.cplett.2019.04.002>, 2019.

-Groß, C. B. M., Dillon, T. J., Schuster, G., Lelieveld, J., and Crowley, J. N.: Direct kinetic study of OH and O₃ formation in the reaction of CH₃C(O)O₂ with HO₂, *The Journal of Physical Chemistry A*, 118, 974–985, <https://doi.org/10.1021/jp412380z>, 2014.

-Glasius, M., Calogirou, A., Jensen, N., Hjorth, J., Nielsen, C.: Kinetic Study of Gas Phase Reactions of Pinonaldehyde and Structurally Related Compounds, *Int. J. Chem. Kinet.* 7; 527–533, [https://doi.org/10.1002/\(SICI\)1097-4601\(1997\)29:7<527::AID-KIN7>3.0.CO;2-W](https://doi.org/10.1002/(SICI)1097-4601(1997)29:7<527::AID-KIN7>3.0.CO;2-W), 1997.

-Heald, C. L.; Kroll, J. H. *The Fuel of Atmospheric Chemistry: Toward a Complete Description of Reactive Organic Carbon*, *Sci. Adv.*, 6, 8967, <https://doi.org/10.1126/sciadv.aay8967>, 2020.

-Hodnebrog, Ø., Aamaas, B., Fuglestad, J. S., Marston, G., Myhre, G., Nielsen, C. J., et al.: Updated global warming potentials and radiative efficiencies of halocarbons and other weak atmospheric absorbers, *Reviews of Geophysics*, 58, e2019RG000691, <https://doi.org/10.1029/2019RG000691>, 2020.

-Hovorka, Š., Vrbka, P., Bermúdez-Salguero, C., Böhme, A., & Dohnal, V.: Air–water partitioning of C₅ and C₆ alkanones: measurement, critical compilation, correlation, and recommended data, *J. Chem. Eng. Data*, 64, 5765–5774, <https://doi.org/10.1021/ACS.JCED.9B00726>, 2019.

-IUPAC. Task Group on Atmospheric Chemical Kinetic. <http://iupac.pole-ether.fr>, 2007.

-Jenkin, M. E., Valorso, R., Aumont, B., and Rickard, A. R.: Estimation of rate coefficients and branching ratios for reactions of organic peroxy radicals for use in automated mechanism construction, *Atmos. Chem. Phys.*, 19, 7691–7717, <https://doi.org/10.5194/acp-19-7691-2019>, 2019.

-Jenkin, M. E., Valorso, R., Aumont, B., Rickard, A. R., and Wallington, T. J.: Estimation of rate coefficients and branching ratios for gas-phase reactions of OH with aliphatic organic compounds for use in automated mechanism construction, *Atmos. Chem. Phys.*, 18, 9297–9328, <https://doi.org/10.5194/acp-18-9297-2018>, 2018.

-Jenkin, M. E., Derwent, R. G., Wallington, T. J.: Photochemical ozone creation potentials for volatile organic compounds: Rationalization and estimation, *Atmos. Environ.* 163, 128–137. <https://doi.org/10.1016/j.atmosenv.2017.05.024>, 2017.

-Jenkin, M. E., Saunders, S. M., and Pilling, M. J.: The tropospheric degradation of volatile organic compounds: a protocol for mechanism development, *Atmos. Environ.*, 31, 81–104, [https://doi.org/10.1016/S1352-2310\(96\)00105-7](https://doi.org/10.1016/S1352-2310(96)00105-7), 1997.

-Kerdouci, J., Picquet-Varrault, B., Doussin, J. F.: Structure–activity relationship for the gas-phase reactions of NO₃ radical with organic compounds: Update and extension to aldehydes, *Atmos. Environ.* 2014, 84, 363–372, <https://doi.org/10.1016/j.atmosenv.2013.11.024>, 2014.

-Kwok, E.S.C., Atkinson, R.: Estimation of hydroxyl radical reaction rate constants for gas-phase organic compounds using a structure-reactivity relationship: An update, *Atmos. Environ.* 29,1685-1695, [https://doi.org/10.1016/1352-2310\(95\)00069-B](https://doi.org/10.1016/1352-2310(95)00069-B), 1995.

-Lanza, B., Jiménez, E., Ballesteros, B., Albaladejo, J.: Absorption cross section determination of biogenic C₅-aldehydes in the actinic region, *Chem. Phys. Lett.*, 454, 184-189, <https://doi.org/10.1016/j.cplett.2008.02.020>, 2008.

-Liu, Q., Gao, Y., Huang, W., Ling, Z., Wang, Z., Wang, X.: Carbonyl compounds in the atmosphere: A review of abundance, source and their contributions to O₃ and SOA formation, *Atmos. Res.*, 274,106184, <https://doi.org/10.1016/j.atmosres.2022.106184>, 2022.

-Mapelli, C., Donnelly, J. K., Hogan, Ú. E., Rickard, A. R., Robinson, A. T., Byrne, F., McElroy, C. R., Curchod, B. F. E., Hollas, D., and Dillon, T. J.: Atmospheric oxidation of new 'green' solvents part II: methyl pivalate and pinacolone, *Atmos. Chem. Phys.*, 23, 7767–7779, <https://doi.org/10.5194/acp-23-7767-2023>, 2023.

-McGillen, M. R., Carter, W. P. L., Mellouki, A., Orlando, J. J., Picquet-Varrault, B. and Wallington T. J.: "Database for the kinetics of the gas-phase atmospheric reactions of organic compounds," *Earth Syst. Sci. Data*, 12, 1203–1216, <https://doi.org/10.5194/essd-12-1203-2020>, 2020.

-Mellouki, A., Wallington, T. J., and Chen, J.: Atmospheric chemistry of oxygenated volatile organic compounds: impacts on air quality and climate, *Chem. Rev.*, 115, 3984–4014, <https://doi.org/10.1021/cr500549n>, 2015.

-NTP (National Toxicology Program). Report on Carcinogens, Fifteenth Edition. Research Triangle Park, NC: U.S. Department of Health and Human Services, Public Health Service, doi.org/10.22427/NTP-OTHER-1003, 2021.

-Pate C. T., Sprung J. L. and Pitts J. N.: Chemical ionization mass spectrum of peroxyacetylnitrate, *J. Mass Spectrom.*, 11, 552-555, <https://api.semanticscholar.org/CorpusID:95293138>, 1976.

~~-Phillips, G. J., Pouvesle, N., Thieser, J., Schuster, G., Axinte, R., Fischer, H., Williams, J., Lelieveld, J., and Crowley, J. N.: Peroxyacetyl nitrate (PAN) and peroxyacetic acid (PAA) measurements by iodide chemical ionisation mass spectrometry: first analysis of results in the boreal forest and implications for the measurement of PAN fluxes, *Atmos. Chem. Phys.*, 13, 1129–1139, <https://doi.org/10.5194/acp-13-1129-2013>, 2013.~~

-Platt, U., Jansen, C.: Observation and role of the free radicals NO₃, ClO, BrO and IO in the troposphere, *Faraday Discuss* 100, 175–198. <https://doi.org/10.1039/FD9950000175>, 1995.

-Prinn, R.G., Huang, J., Weiss, R.F., Cunnold, D.M., Fraser, P.J., Simmonds, P.G., McCulloch, A., Harth, C., Salameh, P., O'Doherty, S., Wang, R.H.J., Porter, L., Miller, B.R.: Evidence for Substantial Variations of Atmospheric Hydroxyl Radicals in the Past Two Decades, *Science*. 292, 1882–1888. doi.org/10.1126/science.1058673, 2001.

-Ren, Y., Wang, J., Grosselin, B., Daele, V., and Mellouki, A.: Kinetic and product studies of Cl atoms reactions with a series of branched ketones, *J. Environ. Sci.*, 71, 271–282, <https://doi.org/10.1016/j.jes.2018.03.036>, 2018.

-Ródenas, M. IR spectrum: FORMALDEHYDE HCHO (Version 1.0) [Data set]. AERIS. <https://doi.org/10.25326/K17C-0762>, 2017.

-Sander, R.: Compilation of Henry's law constants (version 5.0.0) for water as solvent, *Atmos. Chem. Phys.*, 23, 10901–12440, <https://doi.org/10.5194/acp-23-10901-2023>, 2023.

-Saunders, S. M., Jenkin, M. E., Derwent, R. G., and Pilling, M. J.: Protocol for the development of the Master Chemical Mechanism, MCM v3 (Part A): tropospheric degradation of non-aromatic volatile organic compounds, *Atmos. Chem. Phys.*, 3, 161–180, <https://doi.org/10.5194/acp-3-161-2003>, 2003

-Schott, G., Davidson, N.: Shock Waves in Chemical Kinetics: The Decomposition of N₂O₅ at High Temperatures, *J. Am. Chem. Soc.* 80, 1841–1853. <https://doi.org/10.1021/ja01541a019>, 1958.

~~-Singh, S., Hernandez, S., Ibarra, Y., Hasson, A.S.: Kinetics and mechanism of the reactions of n-butanal and n-pentanal with chlorine atoms. *Int. J. Chem. Kinet* 41: 133–141, <https://doi.org/10.1002/kin.20383>, 2009.~~

-Spicer, C.W., Chapman, E.G., Finlayson-Pitts, B.J., Platridge, R.A., Hubbe, J.M., Fast, J.D., Berkowitz, C.M.: Unexpected high concentrations of molecular chlorine in coastal air. *Nature* 394, 353–356. <https://doi.org/10.1038/28584>, 1998.

-Tadic, J. M., Moortgat, G. K., Bera, P. P., Loewenstein, M., Yates, E. L., and Lee, T. J.: Photochemistry and photophysics of n-butanal, 3-methylbutanal, and 3,3 dimethylbutanal: Experimental and theoretical study, *J. Phys. Chem. A*, 116, 5830–5839, <https://doi.org/10.1021/jp208665v>, 2012.

-Tanielyan, S.K. and Augustine, R. L.: Synthesis of 3,3-dimethylbutanol and 3,3-dimethylbutanal, important intermediates in the synthesis of Neotame, *Top Catal.*, 55, 625-630, <https://doi.org/10.1007/s11244-012-9841-z>, 2012.

-Taylor, W.D., Allston, T.D., Moscato, M.J., Fazekas, G.B., Kozlowski, R., Takacs, G.A.: Atmospheric photodissociation lifetimes for Nitromethane, Methyl Nitrite and Methyl Nitrate, *Int. J. Chem. Kinet.* 12, 4, 231–240. <https://doi.org/10.1002/kin.550120404>, 1980.

-Tomas, A., Villenave, E., and Lesclaux, R.: Reactions of the HO₂ radical with CH₃CHO and CH₃C(O)O₂ in the gas phase, *J. Phys. Chem. A*, 105, 3505–3514, <https://doi.org/10.1021/jp003762p>, 2001.

-Tuazon, E.C., Atkinson, R.: A product study of the gas-phase reaction of Isoprene with the OH radical in the presence of NO_x, *Int. J. Chem. Kinet.* 22, 1221–1236, <https://doi.org/10.1002/kin.550221202>, 1990.

-Tuazon, E. C., Leod, H. M., Atkinson, R., and Carter, W. P. L.: α -Dicarbonyl Yields from the NO_x Air Photooxidations of a Series of Aromatic Hydrocarbons in Air, *Environ. Sci. Technol.*, 20, 383–387, <https://doi.org/10.1021/es00146a010>, 1986.

-US EPA. [2024]. Estimation Programs Interface Suite™ for Microsoft® Windows, v 4.11 or insert version used]. United States Environmental Protection Agency, Washington, DC, USA.

-Vereecken, L., and Peeters, J.: A structure–activity relationship for the rate coefficient of H-migration in substituted alkoxy radicals, *Phys. Chem. Chem. Phys.*, 12, 12608–12620, <https://doi.org/10.1039/C0CP00387E>, 2010.

-Vereecken, L., and Peeters, J.: Decomposition of substituted alkoxy radicals—part I: a generalized structure–activity relationship for reaction barrier heights, *Phys. Chem. Chem. Phys.*, 11, 9062–9074, <https://doi.org/10.1039/B909712K>, 2009.

-Vila, J. A., Argüello, G. A., Malanca, F. E.: Kinetics studies of 5-methyl-2-hexanol, 2,2-dimethyl-3-hexanol, and 2,4,4-trimethyl-1-pentanol with chlorine atoms: Photooxidation mechanism of 2,4,4-trimethyl-1-pentanol, *Int. J. Chem. Kinet.*, 52(1), 29-34, <https://doi.org/10.1002/kin.21327>, 2020.

-Wallington, T. J. and Kurylo, M. J.: Flash Photolysis Resonance Fluorescence Investigation of the Gas-Phase Reactions of OH Radicals with a Series of Aliphatic Ketones over the Temperature Range 240–440 K, *J. Phys. Chem.*, 91, 5050–5054, <https://doi.org/10.1021/j100303a033>, 1987.

-Winiberg, F. A. F., Dillon, T. J., Orr, S. C., Groß, C. B. M., Bejan, I., Brumby, C. A., Evans, M. J., Smith, S. C., Heard, D. E., and Seakins, P. W.: Direct measurements of OH and other product yields from the HO₂ + CH₃C(O)O₂ reaction, *Atmos. Chem. Phys.*, 16, 4023–4042, <https://doi.org/10.5194/acp-16-4023-2016>, 2016.

-Xiong, K., Zheng, X., Jiang, M., Gao, D., Wang, F., and Chen [Y*](#).: Phase Equilibrium on Extraction Methylphenols from Aqueous Solution with 3,3-Dimethyl-2-butanone at 333.2 K and 353.2 K, J. Chem. Eng. Data, 63, 7, 2376–2383, <https://doi.org/10.1021/acs.jced.7b00932>, 2018.

-Zhou, X., Zhou, X., Wang, C., Zhou, H.: Environmental and human health impacts of volatile organic compounds: A perspective review, Chemosphere, 313, <https://doi.org/10.1016/j.chemosphere.2022.137489>, 2023.